Temporal Dynamics of Visual Priming and Masking Effects in the Higher Visual Regions of Human Brain

Yasuki Noguchi

Department of Physiological Sciences

School of Life Sciences

The Graduate University for Advanced Studies

2005

Contents

Abstract

When two visual stimuli are sequentially presented with a brief interval, neural responses to those stimuli within the visual areas are known to interact with each other. Although recent brain imaging studies using functional magnetic resonance imaging (fMRI) have investigated neural response changes in those interactions, the temporal aspects of these changes in the human brain are almost unknown, due to the limited temporal resolution of fMRI. Here we used magnetoencephalography (MEG) and studied the temporal dynamics of these neural interaction effects between two visual stimuli.

In the first study, we investigated the 'priming effect', a phenomenon in which neural processing of the first visual stimulus facilitates that of the second. As a neural correlate of this effect, previous fMRI studies have suggested an attenuation of the neural activity to the second stimulus by the existence of the first stimulus, although the detailed temporal changes of this attenuation remain to be elucidated. Focusing on the neural activity in the ventral visual areas related to the shape recognition, we showed that the priming effect induces significant reductions of visual activity both in its strength (neural amplitude) and peak latency. Furthermore, a significant correlation was observed between the shortening of peak latency and behavioral priming effect

(reduction in reaction time, RT decrease), while no correlation could be found between the peak amplitude and RT. These results indicate that (i) the priming effect involves the brain response changes in the temporal domain as well as the response attenuation reported previously, and (ii) the behavioral priming effect (RT decrease) in previous studies is closely correlated with the reduction of peak latency observed presently.

In the second study, we investigated another type of interaction between two visual stimuli: backward masking effect. In this effect, the visibility of the first stimulus (target) is impaired by the second stimulus (mask) presented just after the first. Our experiment using MEG revealed that, as the visibility of the target stimulus was reduced by the mask following it, the neural response to the target in the visual ventral regions showed gradual decreases both in its peak amplitude and peak latency. Furthermore, this decrease in the peak amplitudes was significantly correlated with the behavioral accuracy of the target identification, while the peak latency was not. These results indicate that backward masking simultaneously produces two types of neural changes in ventral visual regions: attenuation of the populational neural activity itself and temporal interruption of this activity by the subsequent mask response. Especially, our data suggest that the response attenuation in higher visual response is a main cause of the perceptual impairment observed in the backward masking paradigm.

General introduction

Previous psychological studies have reported that there are some interaction effects in the human brain between the neural processing of two visual stimuli successively presented. For example, when the same stimulus is repeatedly presented with a brief interval, subjects can detects the second stimulus more rapidly than when two different stimuli are presented (priming effect). On the other hand, when second stimulus appeared just after the offset of the first stimuli, the visibility of the first stimuli is impaired (backward masking effect). Although recent studies of fMRI provided several insights into the brain mechanisms underlying these neural interactions (as described below), a low temporal resolution of fMRI has constrained our understanding of temporal dynamics of neural changes behind these effects. Here we conducted two experiments of MEG, a non-invasive imaging tool with fine temporal resolution. The results would reveal temporal changes in neural activities induced by the priming and backward masking effects between two visual stimuli.

Experiment 1: Priming effect

One common finding in neurophysiological and neuroimaging studies is a reduced neural response to repeated as compared to unrepeated stimuli (Wiggs and

Martin, 1998; Schacter and Buckner, 1998; Henson and Rugg, 2003). Although this attenuation was first reported in inferior temporal neurons of monkeys (Brown et al., 1987; Baylis and Rolls, 1987; Miller et al., 1991; Desimone, 1996; Ringo, 1996), recent studies using positron emission tomography (PET) and fMRI showed that the effect also occurs in various regions of the human brain, including the occipital (Grill-Spector et al., 1999; Kourtzi and Kanwisher, 2000), parietal (Naccache and Dehaene, 2001) and inferior frontal cortices (Raichle et al., 1994; Thompson-Schill et al., 1999; Wagner et al., 2000; van Turennout et al., 2000).

In spite of mounting evidence of the repetition attenuation or priming effect, the temporal profiles of this effect as a neural network has been poorly understood, probably due to the limited temporal resolution of hemodynamic imaging methods such as PET and fMRI. Although a decrease in the blood-oxygen-level dependent (BOLD) signal has been regarded as a sign of this effect in fMRI studies, a previous study indicated that this can arise from at least two types of neural activity (Henson and Rugg, 2003) (Fig. 1). One explanation is a reduced firing rate as a whole neural population in each cortical area (Fig. 1A). This view is strongly supported by many studies of unit cell recordings and the ‘sharpening’ theory propounded by Wiggs and Martin (Wiggs and Martin, 1998). According to this theory, neurons that are not critical for

recognizing an object decreases their responses as the object is repeatedly presented, while those carrying essential information continue to give a robust response. As a result, the mean firing rate as a whole is attenuated by stimulus repetition. On the other hand, a reduction in BOLD responses can also be explained by the response change in the temporal domain: a shortened duration of neural activity (Henson and Rugg, 2003) (Fig. 1B). This account is based on the fact that the hemodynamic response represents the integration of several seconds of neural/synaptic activity, and proven to be possible by a previous neural computation theory (Becker et al., 1997). In this theory, the neural processing network settles to a stable response more quickly in response to a repeated than novel stimulus, because the network connections involved in producing the response have been reinforced by a previous presentation of the same stimulus. Indeed, a recent fMRI study reported results supporting this view (Henson et al., 2002a), although their analysis requires the assumption of a precise linearity of hemodynamics.

In the present study, we used MEG with a high temporal resolution, and measured directly the neural responses underlying the neural adaptation (NA) or priming effect in the human shape perception area (Grill-Spector et al., 1999; Kourtzi and Kanwisher, 2001). As a result, our data supported the integrative model of the response reduction

and temporal acceleration, as shown in the third hypothesis depicted in Figure 1C.

Methods

Subjects.

Ten healthy volunteers participated in the present study (7 males and 3 females). All subjects had normal or corrected-to-normal visual acuity. Informed consent was received from each participant after the nature of the study had been explained. Approval for these experiments was obtained from the ethics committee of the National Institute for Physiological Sciences, Okazaki, Japan.

Stimuli and Task.

One problem with MEG experiments on visual function is that the neuronal signals from the higher visual areas are difficult to be distinguished from those in early visual cortex (such as V1) in most cases, due to the insufficient modeling quality of V1 activities. Since neural responses in the early visual areas are relatively insensitive to the repetition effect compared with those in the later visual areas (Buckner et al., 1998; Schacter and Buckner, 1998), the confounding of early visual signals into MEG data in the present study would obscure the NA effect occurring in higher visual areas. Given

recent studies reporting that V1 area receives a delayed feedback signal from the higher visual cortex at a latency of 190-230 ms (Noesselt et al., 2002; Halgren et al., 2003) in addition to the primary visual input from the thalamus, it would be difficult to exclude the early visual signals on the basis of signal latency. We therefore presented visual stimuli based on our random dot blinking (RDB) technique developed previously (Okusa et al., 1998). With this method, characters are presented in the center of a black-and-white random dot field. Although all dots in the field flicker continuously in the resting state, a subset of dots becomes static during the character presentation period while the other dots remain dynamic (Fig. 2A). This static-dynamic contrast enables observers to perceive the shape of a letter. Since the ratio of white and black pixels is fixed throughout both periods, the mean luminance of the field is always the same. Our previous study has shown that this stimulation paradigm effectively inhibits the neural responses from the V1 area and elicits one simple component of magnetic response at a peak latency of ~300 ms, the signal source of which is estimated to lie in the occipito-temporal area around the fusiform gyrus.

We used the RDB method for sequential presentation of two visual stimuli (letters) in the central visual field of the subjects. All stimuli were presented in a random dot field subtending a visual angle of 6 x 6 degrees with a 60 x 60-dots array on

the projector screen at a viewing distance of 250 cm. For the dynamic texture, each dot (2 x 2 pixel) changed its position within a 3 x 3 pixel area every 16 ms in a pseudo-random manner so as to produce vibrating motion. For the static texture, the dots remained stationary. The ratio of white to black pixels was fixed at 1:3 throughout the whole scanning period.

We used six capital letters (A, O, E, B, K, P) as letter stimuli. Each letter was employed as both S1 (first stimulus) and S2 (second stimulus). The display duration of S1 and S2 was 300 and 500 ms, respectively. The time interval between S1 and S2 (ISI) was either 150, 250 or 350 ms (Fig. 2B), and there were two kinds of trials for each ISI. In 'SAME' trials, the same letter was repeatedly presented as S1 and S2. In 'DIFF' trials, the S1 and S2 letters differed. Because each letter was presented as S1 or S2 in both SAME and DIFF trials at equal times, the difference in brain responses between these two types of trials cannot be attributed to the difference in the visual features of the stimuli presented. Apart from these six conditions (three ISIs x SAME or DIFF), we introduced a control condition in which only S1 was presented for 300 ms (SINGLE condition).

A single scanning session of MEG recordings started with 6 trials of the SINGLE condition during which subjects were instructed to look passively at the letter presented

(no-task period). This period was followed by 72 trials with paired letter stimuli (task period). In this period, stimulus pairs in the six conditions (12 trials for each) were randomly intermixed and subjects were asked to perform a vowel/consonant judgment task with S2, not S1, characters. They were instructed to press one button as quickly as possible when the S2 letter was a vowel (A, O, E), and another button when it was a consonant (B, K, P). All responses were made by the right hand of the subjects. The session ended with another no-task period composed of 6 trials of the SINGLE condition. To prevent the task and no-task periods being confused, cue stimuli showing the switch between the two periods were presented. The numerals '2' and '1' were presented at the beginning and end of the task period, respectively. A scanning session containing 84 trials in total (approximately 5 minutes) was repeated 6 times in one experiment. Every three trials, a brief interval (2 or 5 seconds) was interposed in which subjects were allowed to blink their eyes. Considering the previous results on the repetition attenuation effect (Henson et al., 2000; Henson et al., 2002b), the use of familiar stimuli (letters) and an indirect task (a task that does not require an explicit recollection of previous events) in the present study would highlight the NA in the higher visual regions.

MEG recordings.

The visual-evoked fields (VEFs) were recorded with a helmet-shaped 306-channel detector array (Vectorview, ELEKTA Neuromag, Helsinki, Finland), which comprised 102 identical triple sensor elements. Each sensor element consisted of two orthogonal planar gradiometers and one magnetometer coupled to a multi-SQUID (superconducting quantum interference device) and thus provided three independent measurements of the magnetic fields. In the present study, we analyzed MEG signals recorded from 204-channel planar-type gradiometers. The signals from these sensors are strongest when the sensors are located just above local cerebral sources (Nishitani and Hari, 2002). The MEG signals were recorded with 0.1-200 Hz bandpass filters and digitized at 900 Hz.

Before MEG recordings, four head position indicator (HPI) coils were placed at specific sites on the scalp. To determine the exact head location with respect to the MEG sensors, electric current was fed to the HPI coils and the resulting magnetic fields were measured with the magnetometer. These procedures allowed for alignment of the individual head coordinate system with the magnetometer coordinate system. The locations of HPI coils with respect to the three anatomical landmarks (nasion and bilateral) were also measured using a 3-D digitizer to align the coordinate systems of

MEG with magnetic resonance (MR) images obtained with a 3-Tesla MRI system (Allegra, Siemens). We adopted the head-based coordinate system used in our previous study (Wasaka et al., 2003). The *x* axis was fixed with the preauricular points, the positive direction being to the right. The positive *y* axis passed though the nasion and the *z* axis thus pointed upward.

Data analyses.

The signals in the seven conditions were averaged separately, time-locked to the onset of S1 stimuli. The averaging epoch ranged from 100 ms before to 1200 ms after the S1 onset, and the pre-stimulus period (initial 100 ms) was used as the baseline. Epochs in which signal variation was larger than 3000 fT were excluded from the averaging. For detecting the occipital signals related to letter recognition, we took the sensor of interest (SOI) approach described in the previous MEG study (Liu et al., 2002). Initially, we selected the SOIs in the present study from 204 planar channels according to the following criteria: the peak deflection in the SINGLE condition lies 200-400 ms after the S1 onset, and a significant deflection (> 2SD of the fluctuation level in baseline period of each channel) continues for at least 60 ms centering on the peak latency. These criteria are based on our previous results reporting the fusiform

activation at a latency of ~300 ms (Okusa et al., 1998). An average of 22.2 SOIs were selected for each subject. We then calculated the mean waveform of all SOIs in each subject, after the data on SOIs showing a negative deflection were flipped to match the polarities (Liu et al., 2002). Using the across-SOI timeseries of each subject, we measured three independent parameters to test the repetition effect between SAME and DIFF: peak amplitude, peak latency, and FWHM (full width at half maximum). The FWHM is the temporal interval where the signal amplitude is above 50 % of the peak. Because it is theoretically independent of variation in the vertical amplitude of the MEG waveform, the FWHM corresponds to an index of the temporal duration of neural activity induced in the ventral visual cortex. Regarding the responses to S1, the peak amplitude and latency were defined as a maximum signal strength (and its latency) in the across-SOI waveforms within the time window of –100 ~ 500 ms after the S1 onset. The time window was set at 500 ~ 1200 ms for S2 responses. Once the peak amplitude was determined, we calculated 50 % of the peak for each response waveform (half maximum). The time interval between the first and last time points in which signal strength is above the half maximum was defined as FWHM (full-width at half-maximum) of this waveform.

Apart from the SOI analyses, we estimated the single equivalent current dipole

(ECD) on response waveforms to confirm the anatomical location of VEF sources. We adopted a spherical head model based on individual MR images (Hamalainen et al., 1993). The ECDs best explaining the distribution of the magnetic field over at least 20 channels around the signal maxima were searched by the least square method (Wasaka et al., 2003). We accepted only ECDs that account for at least 80 % of the field variance at the peak.

Results

Figure 3A shows the VEF in the SINGLE condition for one subject. Clear deflections were observed mainly in MEG channels on the lateral sides of both hemispheres. Magnetic responses around the occipital pole were relatively small, indicating that neural responses in the early visual areas were successfully inhibited by the RDB stimulus. Figure 3B shows the superimposed waveform of all SOIs in the same subject. Consistent with our previous study (Okusa et al., 1998), a large component was observed at a latency of ~300 ms. We plotted in Figure 3C the waveform of all conditions in two representative SOIs marked in Figure 3A. Magnetic responses to S2 that have the same polarity as those to S1 were clearly observed in the six conditions with the paired letter presentation, but they were absent in the SINGLE

condition. The S2 response latencies reflected the difference of S2 onset in the three ISI conditions. Within each ISI, the S2 response in the SAME condition appeared to show earlier peak latency (latency at the peak) and smaller deflection than that in the DIFF condition.

The results of dipole analyses indicated that all ECDs (equivalent current dipoles) calculated on MEG signals in the SINGLE condition were estimated in the vicinity of the occipito-temporal cortex around the fusiform gyrus, which also confirmed our previous results (Okusa et al., 1998). In Figure 4A, the mean dipole location of each hemisphere across subjects was shown on the MR image of a representative subject. According to the head-based coordinate system used, the mean (+/- SE, standard error) coordinates were (-31 +/- 9.6, -26 +/- 3.5, 44 +/- 3.0) for left and (35 +/- 3.2, -20 +/- 4.2, 48 +/- 3.1) for right hemispheres. There was no significant difference of ECD locations between the two hemispheres ($P > 0.1$, for all axes). These ECD results could be reinforced by two topography maps depicted over the field of 102 sensor positions in MEG. Figure 4B shows a distribution of 222 SOIs selected from the data of ten subjects and thus, represents how many times each sensor was selected as SOI. We also made another contour map (Fig. 4C) in which mean deflection of MEG waveforms at 300 ms of SINGLE condition are plotted for each sensor position. The

results of both maps indicate that the signal sources of the 300 ms component are located in the bilateral occipital-temporal regions.

We showed in Figure 5 the across-SOI waveforms of one subject (Fig. 5A) and grand mean of 10 subjects (Fig. 5B). In S2 responses, both peak amplitude and peak latency were clearly different between the SAME and DIFF trials in all three ISI conditions. In contrast, S1 responses in the six conditions with a paired stimulus were almost identical although, in the grand mean waveform, peak latency was significantly delayed in the SINGLE condition compared to the other six conditions ($P < 0.05$, t-test), probably due to the lack of a task requirement in the SINGLE condition. To closely investigate the temporal profiles of the response waveforms irrespective of their amplitude differences, we also presented the grand mean timecourses normalized to the S2 peak amplitude of each paired-stimulus condition (Fig. 5C). In all of three ISI conditions, the S2 responses in the SAME trials reach their peak more rapidly than those in the DIFF trials. The SAME responses also precede the DIFF in their signal decreases.

We then examined the NA effect statistically by calculating the three independent parameters on the across-SOI timeseries of each subject: peak amplitude, peak latency, and FWHM (full width at half maximum) of response waveforms (Fig. 6). In each

panel of Figure 6, we employed repeated-measures ANOVA of ISI x repetition (SAME vs. DIFF) with repetition as a within-subject factor. The Mauchly's tests indicated that the sphericity assumption was not rejected in all comparisons. In the S1 response, there was no significant main effect or interaction in any parameters ($P > 0.05$ for all, Fig. 6A, C and E). On the other hand, the peak amplitude and latency of the S2 response showed a significant main effect of repetition ($P < 0.0001$ for both; the other effects were not significant, $P > 0.05$) (Fig. 6B and D). There was, however, no significant effect in the FWHM of the S2 signal ($P > 0.05$, Fig. 6F), although the DIFF trials tended to have a larger FWHM value than the SAME trials (main effect of repetition, $F = 4.037$, $P > 0.05$). In Figure 7, we plotted the repetition effect (DIFF-SAME) of the three indices. One-group t-test applied to each bar demonstrated that the significant effect of repetition (SAME < DIFF) in S2 peak amplitude and latency could be observed in all three ISIs (Figure 7A and B, $P < 0.05$ for all), whereas no repetition effect of FWHM was observed in any ISI conditions (Figure 7C, $P > 0.05$).

Although significant repetition effects were observed in S2 peak amplitude and latency, the signal source of these effects remains unclear, because the source location of the repetition effect (DIFF-SAME) was not directly investigated. We therefore conduced the ECD estimation again, using the DIFF-SAME waveform of each ISI

condition. The across-subject mean and SE of these ECD locations were; ISI 150 (41 +/- 4.5, -24 +/- 4.2, 52 +/- 4.0), ISI 250 (37 +/- 4.8, -15 +/- 5.4, 41 +/- 3.8), ISI 350 (37 +/- 3.8, -21 +/- 5.0, 50 +/- 4.0) for right hemisphere, and ISI 150 (-43 +/- 9.7, -20 +/- 5.9, 48 +/- 5.4), ISI 250 (-27 +/- 7.1, -43 +/- 7.2, 50 +/- 3.8), ISI 350 (-33 +/- 8.2, -29 +/- 10.3, 49 +/- 4.3) for left hemisphere. To examine whether these ECD locations were significantly different from that for the S1 peak, we performed one-way ANOVA with four levels (S1 and three ISI conditions) for each axis and each hemisphere. No significant main effect was observed in all comparisons ($P > 0.05$ for all). These results suggest a common neural generator of the repetition effect and S1 SINGLE component.

Finally, we investigated the relationship between behavioral performance of the vowel/consonant judgment task and MEG waveforms. Subjects performed the task very well and accuracy in the six conditions ranged from 97.5 to 98.3 %. On the other hand, a significant RT reduction in the SAME compared to DIFF condition was observed in all three ISIs (Fig. 8A; main effect of repetition, $P < 0.001$, repeated-measures ANOVA), as was seen in many behavioral results of previous studies (Raichle et al., 1994; Buckner et al., 1998; Thompson-Schill et al., 1999; Wagner et al., 2000; van Turennout et al., 2000; Naccache and Dehaene, 2001). In Figure 8B, results

of correlation analyses between the task RT and the S2 peak latency (Fig. 6D) or S2 FWHM (Fig. 6F) are shown. Whereas peak latency exhibited a high correlation with RT data (r = 0.48, P < 0.0001), no significant correlation was found between FWHM and RT (r = 0.09, P > 0.05). This close relationship between RT and peak latency was also seen when we compared the priming effect (DIFF-SAME) in these two indices (r = 0.35, P = 0.05). These results indicate that behavioral responses are highly predictable based on the latency, but not temporal duration, of the occipito-temporal activation.

Discussion

In the present study, we conducted a macro-level analysis of the temporal profiles of the NA effect in the shape perception area of the human brain. Although brain responses to two rapidly-presented visual stimuli were previously indistinguishable from each other due to the limited temporal resolution of other macro-level imaging techniques such as PET and fMRI, we examined the S1 and S2 responses in the occipito-temporal areas separately by combining MEG recording with the RDB method. In contrast to the S1 response in which no difference was observed between the SAME and DIFF trials, the S2 response showed a clear NA effect both in peak amplitude and peak latency. On the other hand, the temporal width (FWHM) of the S2 response was

not significantly affected by the stimulus repetition.

One previous study using intracranial event-related potential (ERP) reported that the first distinct response in visual ventral areas appears approximately 200 ms after the stimulus onset (Puce et al., 1999). On the other hand, the occipito-temporal responses in the present study were observed at a latency of 300 ms, 100 ms later than that in the intracranial ERP. We suppose that this delay in response latency would be caused by the special characteristics of our RDB stimuli. While letters in the ERP study were defined by the luminance difference from the background, our stimuli were presented through a static-dynamic contrast between letters and background. A recent MEG study (Schoenfeld et al., 2003) showed that the response latency in shape processing areas is variable depending on how the visual stimuli are defined. According to them, visual shape stimuli (squares and rectangles) defined by luminance cues activated a serial processing stream from V1 to lateral occipital (LO) and inferior temporal (IT) regions, whereas shapes defined by motion coherence of random dots (similar but not identical to ours) elicited the activation in MT/V5 before evoking LO and IT responses. As a result, the response latency in LO and IT was delayed for 50-60 ms in response to the motion-defined than luminance-defined shapes, despite the same response latency in early visual areas. Although where in the brain our RDB stimuli are processed is

unclear, it is possible for the RDB letters to be processed in several areas (in the dorsal stream) before reaching occipito-temporal regions, resulting in some delay of activity in the visual ventral pathway.

In Figures 6 and 7, we showed that both peak amplitude and latency in S2 response were significantly modulated by the stimulus repetition. These results, however, may be explained merely by the amplitude reduction, because the decrease in peak amplitude inevitably involves the shortening of peak latency when SAME and DIFF shows the neural response curves with similar shapes. To examine this possibility, we calculated the correlation coefficient between the peak amplitude and peak latency. If the decrease in peak latency is a 'by-product' of the amplitude attenuation, these two values would show a high positive correlation (the smaller the amplitude is, the shorter the latency becomes). The result revealed that only the weak correlation was observed between peak amplitude and latency (r = 0.17, P > 0.05), suggesting that decrease in amplitude and latency occurred independently although these changes appear to occur simultaneously in the grand-average timecourse (Figure 5B). We also investigated the relationship between DIFF-SAME of peak amplitude and latency, only to find that their correlation was not significant again (r = 0.29, P > 0.05). In addition, the peak amplitude was also poorly correlated with the RT data (r =

-0.14, $P > 0.05$), whereas the high correlation was observed between the peak latency and RT as shown in Figure 8B. Our conclusion, therefore, is that the reductions in peak amplitude and peak latency were independent phenomena produced by the stimulus repetition, and RT decreases behaviorally observed was mainly induced by the decrease in peak latency, not peak amplitude.

One characteristic of the present study is that the temporal durations of neural responses were measured by FWHM. It may seem unnatural that no significant difference between SAME and DIFF was observed in FWHM of S2 responses (Figs. 6 and 7), because one would expect a longer processing of DIFF than SAME if the duration of activation were defined by the time interval during which the amplitudes are above a certain criterion (see Fig. 5B). This apparent inconsistency is caused by the fact that the FWHM is determined based on the size of the peak amplitude for each response curve, and thus, is free from the amplitude effects at least theoretically. Indeed, we initially calculated the temporal duration of waveforms by applying the constant criterion (50 % of S1 peak amplitude in the SINGLE condition) to the six conditions with paired stimuli. The result revealed that these measures were highly correlated with the peak amplitudes ($r = 0.62$, $P < 0.0001$), indicating that temporal and amplitude effects are mixed in this index. In contrast, the correlation between peak

amplitude and FWHM is not significant (r = 0.24, P > 0.05), as predicted by the theoretical consideration above. Since our primary purpose is to investigate the temporal dynamics of the neural adaptation effect other than response attenuation, we adopted the FWHM as a better index to measure the temporal duration of waveforms irrespective of their amplitude difference. It may be, however, difficult to argue that the FWHM is completely independent from amplitude effects, because the correlation between them was not zero (0.24).

It should be noted that the repetition interval in the present study is relatively short (150 - 350 ms) compared to those in most previous studies, and therefore, is closely related to the 'neural adaptation' technique used in several recent researches (Grill-Spector et al., 1999; Kourtzi and Kanwisher, 2000; Kourtzi and Kanwisher, 2001). This short ISI also distinguishes our study from previous anatomically-constrained MEG (aMEG) studies (Dhond et al., 2001; Marinkovic et al., 2003) using the longer repetition interval consisted of several intervening items. Indeed, it was suggested that neural response attenuation induced by the immediate stimulus repetition (less than 1 s) is qualitatively different from that involved in long-lag repetition of more than several seconds. For example, the neural adaptation with short ISI may be induced by the response attenuation of the same groups of neurons, rather than the decrease in neural

population encoding the repeated stimuli as assumed in the sharpening theory (Henson, 2003). Although our study revealed the temporal profiles of the NA effect in visual ventral regions, one should attend to the scale of repetition lag for the interpretation of the present results.

There are two neural models that can account for the BOLD signal decrease in response to the repeated compared to unrepeated stimulus: a reduction in mean firing rate (Wiggs and Martin, 1998) and shortened duration of neural activity (Becker et al., 1997; Henson et al., 2002a). The present results strongly favor the integration of these two models. In addition to a decrease in neural activation by the repeated relative to unrepeated stimulus, we found that NA also induced a temporal shift of peak latency (Fig. 6D). Furthermore, this peak latency showed a significant correlation with RT data (Fig. 8B). These results support the shortened duration model which attributes NA to the reduced settling time of the neural processing network (Becker et al., 1997). However, our results also showed that this shortening of settling time does not lead to a significant reduction in the temporal duration of response curve itself, because the FWHM, an index of the temporal width of neural processing, was not significantly modulated by the stimulus repetition. These results indicate that, although NA surely involves a change in the neural response in the temporal domain, this change is

primarily observed as a speeded response of shape perception areas, rather than a temporal shortening of neural response shapes within these areas.

In conclusion, the present study demonstrated that the NA effect in the human visual ventral stream is characterized by both activation reduction and temporal acceleration, and that the decreased rising time in the ventral visual area is a main factor in the reduction in RT observed. Although there are some limitations on the interpretation of our study (e.g. the frequency changes at such as gamma band were omitted in our trial-averaged analysis, which may relate to hemodynamics changes involved in stimulus repetition), the present results should have an impact on future neural computational theories and provide further insight into the visual processing mechanism in the human brain.

Experiment 2: Backward masking effect

When a brief visual stimulus is followed by another stimulus, the perceptivity of the first stimulus could be impaired by the existence of the second (Breitmeyer and Ganz, 1976; Enns and DiLollo, 2000; Kahneman, 1968; Turvey, 1973). This is called backward masking and has attracted the interests of many previous studies on visual mechanisms (Coenen and Eijkman, 1972; Schiller, 1968). An important issue of

primarily observed as a speeded response of shape perception areas, rather than a temporal shortening of neural response shapes within these areas.

In conclusion, the present study demonstrated that the NA effect in the human visual ventral stream is characterized by both activation reduction and temporal acceleration, and that the decreased rising time in the ventral visual area is a main factor in the reduction in RT observed. Although there are some limitations on the interpretation of our study (e.g. the frequency changes at such as gamma band were omitted in our trial-averaged analysis, which may relate to hemodynamics changes involved in stimulus repetition), the present results should have an impact on future neural computational theories and provide further insight into the visual processing mechanism in the human brain.

Experiment 2: Backward masking effect

When a brief visual stimulus is followed by another stimulus, the perceptivity of the first stimulus could be impaired by the existence of the second (Breitmeyer and Ganz, 1976; Enns and DiLollo, 2000; Kahneman, 1968; Turvey, 1973). This is called backward masking and has attracted the interests of many previous studies on visual mechanisms (Coenen and Eijkman, 1972; Schiller, 1968). An important issue of

backward masking is that this effect cannot be simply attributed to the brief duration of the first stimulus (target), because a target with the same duration can be clearly seen when no masking stimulus follows it. Only when the second stimulus (mask) was presented within a brief interval (< 100 ms, usually) after the target, the visibility of the target is reduced and even becomes invisible in appropriate conditions.

Backward masking has been regarded as a powerful way of studying the visual awareness of humans, because physically identical stimulus could be perceivable or not depending on its relationships with the mask, such as spatial positions and temporal lag in stimulus presentation (Enns and DiLollo, 2000). Previous studies have investigated what activation pattern in the brain underlies the visual awareness of the target, by comparing the neural responses when the target is masked and unmasked. As a result, one key region that closely correlates with visual consciousness has been shown to lie in the visual ventral regions related to shape perception or object recognition (Bar et al., 2001; Grill-Spector et al., 2000; Rolls, 2004). Neurophysiological studies on monkeys indicated that the reduced visibility of the masked stimuli is characterized by response changes in inferior temporal neurons to that stimuli (Kovacs et al., 1995; Rolls et al., 1999). Interestingly, at least two types of response change have been reported: a decrease in firing rate encoding the target (attenuation in the spike-frequency scale)

and/or the interruption of target processing by the subsequent mask response (cessation in the temporal scale). The response change in higher visual region has been also recently confirmed by macro-level approaches using fMRI that showed BOLD signal reductions by the masking (Bar et al., 2001; Dehaene et al., 2001). These studies on humans further reported a significant correlation between the ventral activity and recognition of masked stimulus (Bar et al., 2001; Grill-Spector et al., 2000).

Although these fMRI studies revealed a decrease in neural activity in higher visual regions caused by the masking, the temporal profiles of the macro-level masking effect have been difficult to investigate, due to the limited temporal resolution of hemodynamic imaging techniques. For example, the linear characteristics of hemodynamic function (Boynton et al., 1996) indicate that the BOLD response attenuation in previous studies can be theoretically yielded by either a reduction in populational firing rate or a temporal interruption of neural activation, both of which have been already suggested by previous unit cell recordings above. As a result, what pattern of neural response change actually impairs our visual awareness remains to be elucidated. In the present study, we used MEG with a high temporal resolution and directly measured the temporal dynamics of macro-level neural changes involved in backward masking.

Methods

Subjects.

Eleven healthy volunteers participated in the present study. All subjects had normal or corrected-to-normal visual acuity. Informed consent was received from each participant after the nature of the study had been explained. Approval for these experiments was obtained from the ethics committee of the National Institute for Physiological Sciences, Okazaki, Japan.

Stimuli and Task.

As experiment 1, all visual patterns in the current study were presented though the RDB method (Fig. 9A), the random dot field of which subtended a visual angle of 6 x 6 degrees (60 x 60-dots array) on the projector screen at a viewing distance of 250 cm. For the dynamic texture, each dot (2 x 2 pixel) changed its position within a 3 x 3 pixel area every 16.7 ms in a pseudo-random manner so as to produce the vibrating motion. For the static texture, the dots remained stationary. The ratio of white to black pixels was fixed at 1:3 throughout the scanning period. We presently used a type of masking called 'pattern masking' (Enns and DiLollo, 2000; Kovacs et al., 1995), in which the contour of the mask and target are spatially superimposed. The target was a letter

depicted by the RDB method, and either ‘m’ or ‘w’ in the present study (Fig. 9B, left and middle panel). After the target disappeared, the second stimulus (mask, Fig. 9B, right panel) was presented at the same spatial position as the target, although its size (5.6 x 5.6 degrees) was far larger than that of the target (1.5 x 2.1 degrees). The mask pattern was a visual noise consisting of a number of square shapes, which has been shown to be effective for masking the letter stimuli (Dehaene et al., 2001).

As shown in Figure 9C, we set three experimental and two control conditions. In the experimental conditions (upper three diagrams in Fig. 9C), the brief target and mask patterns were sequentially presented, and subjects were asked to report which of two letters appeared before the mask (two choices). The display duration of the target was set at the shortest interval in which a subject can explicitly discriminate ‘m’ from ‘w’ when no masking stimulus follows it, and thus determined for each subject in 16.7-ms steps (127 ms on average across 11 subjects). The mask duration, on the other hand, was fixed at 500 ms. The three conditions were defined according to the three durations of the inter-stimulus interval (ISI) between the target offset and mask onset: 0, 150, and 300 ms (ISI 0, ISI 150, and ISI 300 conditions, respectively). As the ISI becomes shorter, the backward masking effect should increase and the task accuracy should come to near a chance level (50 %). Apart from these three conditions, we also

measured the brain responses when only either the target or mask was presented with the same temporal duration and timing as the ISI 0 condition (TGT and MSK, respectively). Trials in these two conditions were randomly intermixed in a control period and the subjects' task in this period was to report which of three stimuli ('m', 'w', or mask) was shown in the field (three choices).

The session started with 16 trials of the single-stimulus conditions during which one of three stimuli (m, w, or mask) was presented alone (control period). In this period, subjects were asked to report which of three stimuli was presented (forced choice). This period was followed by 48 trials of paired-stimuli conditions, during which stimulus pairs in the three ISI conditions (16 trials for each) were randomly intermixed (experimental period). The subjects' task in this period was to judge whether the target was 'm' or 'w' (forced choice), neglecting the mask. Note that the task in this period was two-choices whereas it was three-choices in the single-stimulus epoch. The session ended with another control period composed of 16 trials of the control period. To prevent the single-stimulus and paired-stimuli periods being confused, cue stimuli showing the switch between the two periods were presented. The numerals '2' and '1' were presented at the beginning and end of the paired-stimuli period, respectively. A scanning session containing 80 trials in total (approximately 5

minutes) was repeated 6 times in one experiment, resulting in an average of 96 trials per condition at maximum. Subjects made all responses by pressing the buttons with their right hand. Due to a technical problem, the behavioral data of one of 11 subjects could not be recorded. Every four trials, a brief interval (2 or 5 seconds) was interposed in which subjects were allowed to blink their eyes.

MEG Recordings.

The VEFs (visual-evoked fields) were recorded with the same MEG system in experiment 1, and we used 204-channel planar-type gradiometers in this system. The neuromagnetic signals were measured with 0.1-200 Hz band-pass filters and digitized at 600 Hz.

Data Analyses.

The signals in the five conditions were averaged separately, time-locked to the onset of the target stimuli. The averaging epoch ranged from 200 ms before to 1300 ms after the target onset, and the pre-stimulus period (initial 200 ms) was used as the baseline. To avoid the confounding of the response-related motor-evoked fields into MEG data, subjects were instructed to press the button after the offset of each averaging

epoch, which was cued by the stopping of dynamic noise in the whole field. Epochs in which signal variation was larger than 3000 fT/cm were excluded from the averaging. For detecting the occipito-temporal signals related to shape perception, we took the SOI approach used in the previous experiment. Two criteria for the selection of SOIs (identical to those in the experiment 1) were applied to the VEFs of MSK condition in the present study. An average of 20.5 SOIs were selected for each subject. We then calculated the mean waveform of all these sensors (across-sensor waveform) for each condition of each subject, after the data on sensors showing a negative deflection were flipped to match the polarities of all sensors (Liu et al., 2002). For a reliable measurement of the peak amplitudes and latencies in these waveforms, a temporal 15-point moving average was applied before searching their peaks. We also conducted correlation analyses between these MEG measures and conscious recognition rate of subjects (Fig. 16). The changes in behavioral accuracy of target identification across four conditions (TGT, ISI 0, ISI 150, ISI 300) were compared with those in peak amplitude and latency of neural responses to the target.

Apart from the sensors-based analyses, we estimated the single equivalent current dipole (ECD) on MEG waveforms to confirm the anatomical location of VEF sources. As in the previous study, the spherical head model and least square method were used to

search ECDs accounting for at least 80 % of the field variance over at least 20 channels.

Results

Behavioral data.

Task accuracies (%) in the three ISI (paired-stimuli) conditions were 69.3 +/- 6.1, 73.6 +/- 5.6, and 78.2 +/- 4.4 for ISI 0, 150, and 300, respectively (mean +/- standard error, SE). The repeated-measured ANOVA revealed a significant main effect of ISI ($F = 7.17$, $P < 0.01$), and, according to the post-hoc test with Bonferroni correction, a robust difference was observed between ISI 0 and ISI 300 ($P < 0.05$, Fig. 10). These results demonstrated a significant backward masking effect in the present study being distinct in the shorter ISI condition. On the other hand, the accuracies (%) in single-stimulus conditions were 75.6 +/- 5.0 (TGT) and 94.7 +/- 2.9 (MSK). Although accuracy in TGT tend to be smaller than that in ISI 300 partly due to the lower chance level of the task in single-stimuli period (33 %) than paired-stimuli period (50 %), no significant difference was observed between TGT and ISI 300 ($t = 1.34$, $P > 0.2$) or between TGT and ISI 150 ($t = 1.34$, $P > 0.2$). In contrast, the TGT condition showed a higher accuracy than the ISI 0 condition ($t = 3.10$, $P < 0.05$), confirming the robust masking effect in the shortest ISI condition.

Neuromagnetic waveforms in higher visual areas

Figure 11A shows the VEFs in the MSK condition for one subject. Although the visual stimuli evoked clear neuromagnetic responses in several MEG sensors, these responses were mainly observed on lateral sides of both hemispheres. The VEFs around the occipital pole were relatively small, indicating that magnetic responses in early visual areas were successfully inhibited by the RDB method. To detect the activity in occipito-temporal regions, we selected a subset of channels for each subject, based on their peak latency and temporal duration of a significant deflection in the MSK condition waveforms. In Figure 11B, we showed the superimposed waveforms of all selected sensors in the same subject. Consistent with our previous data (Okusa et al., 1998), the mask stimulus presented through the RDB method induced a single large component at a latency of 300-400 ms after the stimulus onset. Some sensors had positive deflections while the other showed negative.

The single dipole analysis performed on each hemisphere indicated that all ECDs calculated on this 300-400 ms component were estimated in the vicinity of the occipito-temporal cortex around the fusiform gyrus. In Figure 12A, the mean dipole locations across subjects were plotted on a MR image of a representative subject. According to the head-based coordinate system we used (Wasaka et al., 2003), the mean

(+/- SE) dipole coordinates were (33 +/- 4.0, -24 +/- 5.2, 46 +/- 3.5) for the right hemisphere and (-33 +/- 9.0, -25 +/- 1.3, 46 +/- 4.4) for the left. There was no significant difference in the mean ECD locations between the two hemispheres ($P > 0.05$, for all axes). We also investigated the signal source location of TGT waveforms. No significant difference was observed between the ECD coordinates in the MSK and TGT conditions ($P > 0.05$, for all axes of both hemispheres). These ECD results could be reinforced by another topography map depicted over the field of 102 sensor positions in MEG (Figure 12B). This map shows a distribution of 225 sensors selected for the analyses of the occipito-temporal activation in 11 subjects and thus, represents how many times each sensor was selected for the analyses. Most of the selected sensors were centered on the bilateral occipital-temporal regions in each hemisphere, although some sensors were located in more anterior regions especially in the right hemisphere.

Sensor waveforms in masked and unmasked conditions

We then calculated the mean waveform of all selected sensors (across-sensor waveforms) in each subject, after the waveforms with a negative deflection were flipped to match the polarities of all sensors. Figure 13 shows the across-sensor waveforms of five conditions in two subjects and grand mean of 11 subjects. Although the duration

of TGT stimuli were different across subjects (e.g. 100 ms for Subject 1, and 150 ms for Subject 2), the TGT and MSK conditions produced a single large response in the occipito-temporal areas in both cases (Fig. 13, upper panels). The signal peaks in the TGT condition were earlier and smaller than those in the MSK condition, reflecting the stimulus onset asynchrony (SOA) and visual feature differences between the target and mask. In contrast, the visual stimuli in the three ISI conditions produced sensor waveforms with two peaks, the second peak of which reflected the presentation timing of the mask stimulus (Fig. 13, lower panels). These two peaks were clearly seen especially in the single-subject level (in the grand-average, the separation of peaks became somewhat unclear, probably due to the variability of the onset timing of target and mask across subjects). In the ISI 0 condition, however, the magnetic responses to the target and mask were merged indistinguishably due to their temporal adjacency.

We therefore isolated the target response in paired-stimuli conditions by subtracting the MSK responses (thick black lines in Fig. 13) from each of three ISI waveforms (lower panels in Fig. 13). Considering the onset differences of the mask stimuli among the three paired-stimuli conditions, the MSK time series was temporally shifted by 150 and 300 ms for the subtraction from ISI 150 and 300 waveforms, respectively. The results are shown in Figure 14A (left panel). In the ISI 300

condition, the target stimulus yielded similar response waveforms to the TGT condition where no successive stimulus was presented, indicating that the neural responses to the target could be successfully modeled by the subtraction. There was indeed no significant difference in peak amplitude or latency between the TGT and subtracted ISI 300 waveforms (peak amplitude: $t = 1.48$, $P > 0.05$, peak latency: $t = 0.07$, $P > 0.05$, Fig. 14B). The waveform in the ISI 150 condition also showed a similar response, although its amplitude and latency became smaller than those in ISI 300. On the other hand, the target waveforms in the ISI 0 condition in which a distinct masking effect was behaviorally observed showed much smaller responses than those in the other three conditions. Moreover, the latency of the peak appeared to be shorter as the ISI decreased, indicating that the neural response in the masked conditions was temporally interrupted and began to return to the baseline more quickly. This latency acceleration was clearly seen when individual differences in response latency were partly corrected (Fig. 14A, right). In this panel, the grand-mean time course were calculated after the peaks of ISI 0 – MSK waveforms were temporally aligned across subjects to reduce the inter-subject variability of peak latency. Statistical comparisons in Figure 14B revealed that there were significant differences among the four conditions both in peak amplitude and in peak latency. For peak amplitude, repeated-measured ANOVA with

the Huynh-Feldt correction indicated a main effect of conditions ($F = 29.56$, $P < 0.001$), with significant differences between ISI 0 and the other three conditions ($P < 0.01$ for all) and between ISI 150 and TGT conditions ($P = 0.001$) (Bonferroni post-hoc test). The peak latency also showed a significant main effect ($F = 4.37$, $P < 0.05$), although this effect was less distinct than that of peak amplitude and a significant difference was only observed between ISI 0 and 300 ($P < 0.05$) after the correction for multiple comparisons.

The crucial role in response amplitude for the conscious recognition

We then investigated the relationship between behavioral accuracy and the two MEG measures (Fig. 15). The changes in peak amplitude of sensor waveforms had a strong correlation with accuracy data ($r = 0.56$, $P = 0.001$), whereas no significant correlation was observed between peak latency and accuracy ($r = -0.15$, $P > 0.05$). The correlation between peak amplitude and latency was also not significant ($r = -0.05$, $P > 0.05$), suggesting that these two MEG measures were independent of each other. These results indicated that the conscious recognition of the target stimulus is highly predictable based on the peak amplitude, not peak latency, of the neural responses in occipito-temporal regions.

The importance in response amplitude for the recognition of the target was also demonstrated in another analyses comparing correct and incorrect trials in ISI 0 condition (Fig. 16A). In this figure, we contrasted the neural waveforms when subjects could report correctly the target stimuli (thick line) with those when they could not (thin line). Because the number of correct trials (69.3 %) was larger than that in incorrect trials (30.7 %), we paired each incorrect trial with the temporally closest correct trial of the same subject (thus the analyses were done on subset of correct trials and the remains were omitted). The results revealed that the brain response to the target showed significantly larger peak amplitude in correct than incorrect trials (left in Fig. 16B, t =2.86, $P < 0.05$). On the other hand, there was no significant difference in peak latency, although the latency of correct trials tended to be longer than that of incorrect trials (right in Fig. 16B, $t = 1.40$, $P > 0.2$).

Comparison of neural responses in occipito-temporal and anterior temporal regions

The topography map of selected sensors (Fig. 12B) showed that, although most sensors for the present analyses were concentrated on bilateral occipito-temoral areas, some were found in more anterior regions particularly in the right hemisphere. According to our ECD estimation, the signal source of these anterior activities was

located in the anterior part of inferior temporal region, which indicates a possibility that neural responses in two different areas (occipito-temporal and anterior temporal regions) were confounded in the analyses above. We therefore classified our sensors into two groups and analyzed their data separately (Fig. 17). As a result, the reductions in peak latency and amplitude (reported in Fig. 14) were found to be significant in both regions (Fig. 17B - D). These data suggest that the neural changes in amplitude and latency induced by the masking actually occurred in an extensive region over the occipital and temporal lobes. Additionally, we compared the data of SOIs in right vs. left hemispheres. Significant reductions in peak amplitude and latency were seen in both hemispheres (not shown).

Discussion

In the present study, we investigated the brain responses related to shape perception, and examined how backward masking affected these neural activities. Our RDB method enabled us to focus on the neural responses to the target in the higher visual areas. This may be also due to the mask-dominant responses in early visual areas as reported in a previous study (Bar et al., 2001). The strong neural responses to the mask in the early visual areas would make the target responses in the same regions

relatively weaker than usual, leading to the successful isolation of target responses in the higher visual regions. As the behavioral accuracy of the task decreased, the target response showed significant reductions both in peak amplitude and latency, indicating that backward masking produces neural response changes in the temporal domain as well as activation attenuation. However, the decrease in peak amplitude was more distinct than that in peak latency, and showed a significant correlation with the behavioral accuracy.

The RDB method and backward making paradigm

One feature of the present study is that the target duration (127 ms on average) was much longer than those in previous studies (several tens of milliseconds). This was caused by the fact that our target stimuli were presented via the RBD method where letters are defined by the static-dynamic contrast of the random dots, not the difference in luminance from the background. Previous neurophysiological studies indicated that a visual stimulus defined by non-luminance attributes has a lower visibility than luminance-defined stimuli, whereas the neural responses in early visual areas to the non-luminance-defined are much smaller than those to the luminance-defined type (Chaudhuri and Albright, 1997; Marcar et al., 2000). While our RDB methods enabled

us to focus on the neural responses in the higher visual cortex, the low visibility of the RDB letters also raised the detection threshold of the visual stimuli, resulting in a longer duration of the target stimulus. The behavioral data in Figure 10, however, indicate that there was a significant backward masking effect as observed in many previous studies that becomes distinct in shorter ISI conditions. This monotonic decrease in the visibility of the target is one of the characteristics in the pattern masking we employed in the present study, whereas the another types of backward masking, the metacontrast masking, shows a non-monotonic, U-shaped change in the target visibility. (Enns and DiLollo, 2000)

Linearity of the target and mask responses

One potential criticism for our data is the use of subtraction method to estimate the target MEG responses from the MSK and three ISI waveforms. Because this procedure assumes the linearity of the target and mask responses, the subtracted waveforms might not accurately reflect the neural responses to the target if the MEG responses to two stimuli cumulate non-linearly. In particular, this problem has a serious influence on the interpretation of latency reduction in our data (Fig. 14B, right). Given that the mask induced MEG responses long before 300 ms after its onset (Fig.

13), it is possible especially in ISI 0 condition that the mask and target responses were temporally overlapped before the target response reached its peak. In such a case, the subtraction procedure itself might produce the decrease in peak latency along with the ISI by cutting off the later parts of the target response. Some aspects of our data, however, suggest that this was not the case in the present study. First, as shown in the right panel in Fig. 14B (and two panels in Fig. 17D), the largest reduction in peak latency was always observed between ISI 300 and ISI 150 conditions, rather than between ISI 150 and ISI 0. Because the peaks of target response in ISI 150 and ISI 300 conditions were clearly separated from those of mask response in most subjects (Fig. 13, lower panels), the reduction in peak latency between these two conditions were at least difficult to be explained by cutting-off effect involved in the subtraction. Second, if the shortening of peak latency was simply due to the cutting-off of later parts of the target responses, it is predicated that the initial part of target response was not affected by the subtraction and thus invariant across four conditions, even if the later part was chopped off by the subtraction. The ISI 0 waveform in Figure 14A, however, began to dissociate from the other three conditions at a relatively early stage around 200 ms after the target onset.

There was some other evidence supporting the linearity assumption in the present

analyses. For example, our results in ISI 300 – MSK waveform (Fig. 14A, red lines) indicated that, when no masking effect could be observed behaviorally, the target responses estimated by the subtraction were very similar to that in target alone condition (TGT). There was indeed no significant difference in peak amplitude or latency between the TGT and subtracted ISI 300 waveforms ($P > .05$ for both). These results suggest that the mask responses in three ISI conditions can be successfully modeled by the waveform in the mask alone condition (MSK). Furthermore, a significant correlation could be observed between behavioral accuracy data and peak amplitude of the target waveforms (Fig. 15). Although we pooled the peak amplitude and accuracy data in four conditions (TGT, ISI 0, 150, and 300) in Figure 15, the correlation remained significant even when only the data in three ISI conditions were used ($r = 0.57$, $P < .001$). This close relationship between subtracted MEG amplitudes and conscious recognition rate of subjects would be difficult to be observed if the MEG waveforms were seriously distorted by the subtraction procedure. Indeed, a previous study has shown that neural activity covarying with the recognition rate is one of the major characteristics of fusiform regions (Bar et al., 2001). We thus concluded that the subtraction method could be basically applicable to MEG waveforms, at least to estimate their peak amplitudes and latencies to the target stimuli.

Neural mechanism underlying the reduction in peak latency and amplitude

Although we found a significant influence of masking on peak latency of the neural signals in higher visual areas, this change in the response latency needs to be interpreted cautiously. Our MEG study of the priming found that the reduction in peak latency was also observed in the neural adaptation paradigm (Bar, 2001; Henson, 2003; Kourtzi and Kanwisher, 2001) where visual neural processing is facilitated by the repetitive presentation of the same visual stimulus. When we compared the neural responses to the repeatedly-presented letters with those in the first presentation, the peak latency in occipito-temporal areas to the repeated letters were significantly shortened than non-repeated letters. Accordingly, the reaction time (RT) of the vowel-consonant judgment task performed on the letter was also significantly reduced in the repeated than non-repeated conditions. Since these reductions in peak latency and the behavioral RT were significantly correlated, we concluded that the latency reduction in higher visual regions reflects a 'facilitation' of the neural processing due to the repetitive presentation of the same stimulus. The similar kind of latency shortening has been also reported in the neurophysiological study on monkeys (Li et al., 1993) (see Bar, 2001 for a theoretical account). On the other hand, the reduction of peak latency in the present study cannot be explained by this neural 'facilitation', because it became

most distinct when the perceptivity of the visual stimulus was significantly impaired (ISI 0 condition). Therefore, our interpretation of the latency change observed here is an 'interruption' of the target response by the subsequent mask response. In the shorter ISI condition, the neural processing of the target would be more susceptive to the disturbance by the mask response and begin to decrease more quickly to the baseline level, resulting in a reduction of the peak latency. The possibility of this temporal interruption indeed has been suggested by several previous studies of unit cell recording in monkeys (Kovacs et al., 1995; Rolls et al., 1999).

Another neural change found to be implicated in backward masking is a decrease in peak amplitude of the target response, which would reflect a reduction in the mean firing rate of higher visual neurons in ventral regions. The reduced excitability of each neuron should lower the probability of the synchronized activity between them that is necessary for the generation of strong MEG signals (Hamalainen et al., 1993; Lounasmaa et al., 1996), leading to a significant reduction in peak amplitude as a whole. This reduction in peak amplitude is consistent with the previous feedforward inhibition model (Breitmeyer, 1984) that assumes an inhibitory influence of the mask on the neural signal evoked by the target stimulus. An important finding in the present study is that this amplitude attenuation was more distinct than the latency acceleration and

showed a significant correlation with the behavioral accuracy of the target identification. These results indicate that, although backward masking elicits a neural response change in both peak amplitude and peak latency, the former has a crucial role in the conscious perception of the target stimulus, at least in the ISI range (0 – 300 ms) and at the target duration used in the present study.

Backward masking effect in other brain regions

It should be noted that the results in the current study do not deny the backward masking effect in brain regions other than the higher visual cortex. Several previous studies have shown that the backward masking involves the target response interruption in V1 by the subsequent mask activation in the same region (Lamme et al., 2002; Macknik and Livingstone, 1998). Although initial target responses in V1 were never affected by the mask response following it, the mask stimuli suppress the after-discharge of the target responses (thought to be the 'recurrent signals' fed backwardly from the higher visual area), which leads to the severe impairment of the conscious recognition of the target. Another group of studies have reported that the masking of the emotional visual stimuli changed the hemispheric dominance of the amygdala activation (Morris et al., 1998; Morris et al., 1999). While a significant

neural response was observed in the left amygdala to the unmasked angry face, the masked presentation of the same stimulus produced the enhanced neural activity in the right amygdala. One possible reason for this diversity of brain regions related to visual masking may be a difference in masked stimuli among previous studies. The two studies above (Lamme et al., 2002; Macknik and Livingstone, 1998) reporting the masking effect in V1 used texture patterns or rectangle bars as target stimuli, whereas they were replaced by the emotional faces in Morris et al., 1998. Although the present study focused on the response change in higher visual regions to visual characters and this is the main feature of our study compared to the previous EEG (Brazdil et al., 1998; Dehaene et al., 1998; Summerfield et al., 2002; Williams et al., 2004) and MEG (Vanni et al., 1996) studies on the visual masking, the temporal dynamics of responses changes in other brain regions under the various types of visual masking should be further studied in future researches.

In conclusion, this is the first macro-level study on the temporal profiles of the backward masking effect in the higher visual regions of the human brain. The present study reported two types of neural changes induced by backward masking: reduction in peak amplitude and shortening of peak latency in higher visual regions. The former results supports an attenuation account of the masking effect that assumes an inhibitory

influence of the mask on the neural signal strength (maximum spike frequency) evoked by the target stimulus, while the latter is consistent with an interruption theory hypothesizing the temporal cessation of target processing by the mask. Our results therefore provided an integrative model of previous two hypotheses. Regarding the cortical mechanisms, we presume that the inhibitory neural inputs to the target response in higher visual regions produced by the mask response play an important role in both types of neural changes. Although it is unclear whether the mask response affects the target response via a bottom-up pathway from early to higher visual areas or lateral inhibition (Rolls et al., 1999) within the higher visual area, the early component of this mask response can influence the response strength itself of the target response (the reduction in peak amplitude), while the later component would interrupt the sustaining neural response to the target (the shortening of peak latency). These interpretations, however, do not go beyond a speculation presently and further investigations are needed to elucidate the detailed mechanism of backward masking.

General discussion

In the present two studies, we used MEG and investigated the temporal changes in neural activity induced by the visual priming or backward masking effects. The

results revealed that both effects produced significant neural changes in the temporal domain, as well as intensity changes of neural activation that were previously reported by many fMRI studies. Our studies, therefore, emphasize an importance of high-temporal-resolution approach to higher cognitive functions of human brain in the future researches. Furthermore, one common finding in the present two experiments was that both priming and masking effects involved the neural changes in the higher visual areas of the ventral pathway. This suggests that the two different types of interactions (facilitative and inhibitive ones) between two stimuli share the same neural substrate within occipito-temporal regions, which is consistent with the previous psychological studies reporting the implicit priming effect. In the implicit priming, the presentation of target stimulus, which is backwardly masked by the subsequent mask stimulus, has a significant facilitative effect on the processing of the mask stimulus. This interaction between priming and masking effects can be easily predicted if the two effects have a common neural substrate.

Although we currently focused on two effects seen in paired visual stimuli, previous psychological studies have reported many other phenomena that would affect the temporal dynamics of neural activity, such as forward masking or perceptual learning effects. By applying several techniques in the present studies (e.g. RDB

methods or SOI analysis) to these fields, future MEG and EEG studies would provide new insights into the temporal aspect of human brain dynamics and bridge the gap between electrophysiological studies on monkeys and fMRI studies on humans.

Acknowledgements

I would like to express my gratitude to professor Ryusuke Kakigi for his generosity and moral support throughout all this study.

I am also very grateful for technical assistance from Dr. T. Okusa, Dr. M. Hoshiyama, Dr. Y. Kaneoke, Dr. K. Inui, Dr. S. Watanabe, Mr. Y. Takeshima, and Mr. O. Nagata in Department of Integrative Physiology, National Institute for Physiological Sciences, Okazaki, Japan.

References

Bar M (2001) Viewpoint dependency in visual object recognition does not necessarily imply viewer-centered representation. J Cogn Neurosci 13:793-799.

Bar M, Tootell RB, Schacter DL, Greve DN, Fischl B, Mendola JD, Rosen BR, Dale

methods or SOI analysis) to these fields, future MEG and EEG studies would provide new insights into the temporal aspect of human brain dynamics and bridge the gap between electrophysiological studies on monkeys and fMRI studies on humans.

Acknowledgements

I would like to express my gratitude to professor Ryusuke Kakigi for his generosity and moral support throughout all this study.

I am also very grateful for technical assistance from Dr. T. Okusa, Dr. M. Hoshiyama, Dr. Y. Kaneoke, Dr. K. Inui, Dr. S. Watanabe, Mr. Y. Takeshima, and Mr. O. Nagata in Department of Integrative Physiology, National Institute for Physiological Sciences, Okazaki, Japan.

References

Bar M (2001) Viewpoint dependency in visual object recognition does not necessarily imply viewer-centered representation. J Cogn Neurosci 13:793-799.

Bar M, Tootell RB, Schacter DL, Greve DN, Fischl B, Mendola JD, Rosen BR, Dale

AM (2001) Cortical mechanisms specific to explicit visual object recognition. Neuron 29:529-535.

Baylis GC, Rolls ET (1987) Responses of neurons in the inferior temporal cortex in short term and serial recognition memory tasks. Exp Brain Res 65:614-622.

Becker S, Moscovitch M, Behrmann M, Joordens S (1997) Long-term semantic priming: a computational account and empirical evidence. J Exp Psychol Learn Mem Cogn 23:1059-1082.

Boynton GM, Engel SA, Glover GH, Heeger DJ (1996) Linear systems analysis of functional magnetic resonance imaging in human V1. J Neurosci 16:4207-4221.

Brazdil M, Rektor I, Dufek M, Jurak P, Daniel P (1998) Effect of subthreshold target stimuli on event-related potentials. Electroencephalogr Clin Neurophysiol 107:64-68.

Breitmeyer B (1984) Visual masking: An integrative approach. Oxford: Clarendon Press.

Breitmeyer BG, Ganz L (1976) Implications of sustained and transient channels for theories of visual pattern masking, saccadic suppression, and information processing.

Psychol Rev 83:1-36.

Brown MW, Wilson FA, Riches IP (1987) Neuronal evidence that inferomedial temporal cortex is more important than hippocampus in certain processes underlying recognition memory. Brain Res 409:158-162.

Buckner RL, Goodman J, Burock M, Rotte M, Koutstaal W, Schacter D, Rosen B, Dale AM (1998) Functional-anatomic correlates of object priming in humans revealed by rapid presentation event-related fMRI. Neuron 20:285-296.

Chaudhuri A, Albright TD (1997) Neuronal responses to edges defined by luminance vs. temporal texture in macaque area V1. Vis Neurosci 14:949-962.

Coenen AM, Eijkman EG (1972) Cat optic tract and geniculate unit responses corresponding to human visual masking effects. Exp Brain Res 15:441-451.

Dehaene S, Naccache L, Cohen L, Bihan DL, Mangin JF, Poline JB, Riviere D (2001) Cerebral mechanisms of word masking and unconscious repetition priming. Nat Neurosci 4:752-758.

Dehaene S, Naccache L, Le Clec'H G, Koechlin E, Mueller M, Dehaene-Lambertz G, van de Moortele PF, Le Bihan D (1998) Imaging unconscious semantic priming.

Nature 395:597-600.

Desimone R (1996) Neural mechanisms for visual memory and their role in attention. Proc Natl Acad Sci U S A 93:13494-13499.

Dhond RP, Buckner RL, Dale AM, Marinkovic K, Halgren E (2001) Spatiotemporal maps of brain activity underlying word generation and their modification during repetition priming. J Neurosci 21:3564-3571.

Enns JT, DiLollo V (2000) What's new in visual masking? Trends Cogn Sci 4:345-352.

Friston KJ, Fletcher P, Josephs O, Holmes A, Rugg MD, Turner R (1998) Event-related fMRI: characterizing differential responses. Neuroimage 7:30-40.

Grill-Spector K, Kushnir T, Edelman S, Avidan G, Itzchak Y, Malach R (1999) Differential processing of objects under various viewing conditions in the human lateral occipital complex. Neuron 24:187-203.

Grill-Spector K, Kushnir T, Hendler T, Malach R (2000) The dynamics of object-selective activation correlate with recognition performance in humans. Nat Neurosci 3:837-843.

Halgren E, Mendola J, Chong CD, Dale AM (2003) Cortical activation to illusory

shapes as measured with magnetoencephalography. Neuroimage 18:1001-1009.

Hamalainen M, Hari R, Ilmoniemi R, Knuutila J, Lounasmaa OV (1993) Magnetoencephalography-theory, instrumentation, and applications to noninvasive studies of the working human brain. Rev Mod Phys 65:413-497.

Henson R, Shallice T, Dolan R (2000) Neuroimaging evidence for dissociable forms of repetition priming. Science 287:1269-1272.

Henson RN (2003) Neuroimaging studies of priming. Prog Neurobiol 70:53-81.

Henson RN, Price CJ, Rugg MD, Turner R, Friston KJ (2002a) Detecting latency differences in event-related BOLD responses: application to words versus nonwords and initial versus repeated face presentations. Neuroimage 15:83-97.

Henson RN, Rugg MD (2003) Neural response suppression, haemodynamic repetition effects, and behavioural priming. Neuropsychologia 41:263-270.

Henson RN, Shallice T, Gorno-Tempini ML, Dolan RJ (2002b) Face repetition effects in implicit and explicit memory tests as measured by fMRI. Cereb Cortex 12:178-186.

Kahneman D (1968) Method, findings, and theory in studies of visual masking. Psychol

Bull 70:404-425.

Kourtzi Z, Kanwisher N (2000) Cortical regions involved in perceiving object shape. J Neurosci 20:3310-3318.

Kourtzi Z, Kanwisher N (2001) Representation of perceived object shape by the human lateral occipital complex. Science 293:1506-1509.

Kovacs G, Vogels R, Orban GA (1995) Cortical correlate of pattern backward masking. Proc Natl Acad Sci U S A 92:5587-5591.

Lamme VA, Zipser K, Spekreijse H (2002) Masking interrupts figure-ground signals in V1. J Cogn Neurosci 14:1044-1053.

Li L, Miller EK, Desimone R (1993) The representation of stimulus familiarity in anterior inferior temporal cortex. J Neurophysiol 69:1918-1929.

Liu J, Harris A, Kanwisher N (2002) Stages of processing in face perception: an MEG study. Nat Neurosci 5:910-916.

Lounasmaa OV, Hamalainen M, Hari R, Salmelin R (1996) Information processing in the human brain: magnetoencephalographic approach. Proc Natl Acad Sci U S A 93:8809-8815.

Macknik SL, Livingstone MS (1998) Neuronal correlates of visibility and invisibility in the primate visual system. Nat Neurosci 1:144-149.

Marcar VL, Raiguel SE, Xiao D, Orban GA (2000) Processing of kinetically defined boundaries in areas V1 and V2 of the macaque monkey. J Neurophysiol 84:2786-2798

Marinkovic K, Dhond RP, Dale AM, Glessner M, Carr V, Halgren E (2003) Spatiotemporal dynamics of modality-specific and supramodal word processing. Neuron 38:487-497.

Miller EK, Li L, Desimone R (1991) A neural mechanism for working and recognition memory in inferior temporal cortex. Science 254:1377-1379.

Morris JS, Ohman A, Dolan RJ (1998) Conscious and unconscious emotional learning in the human amygdala. Nature 393:467-470.

Morris JS, Ohman A, Dolan RJ (1999) A subcortical pathway to the right amygdala mediating "unseen" fear. Proc Natl Acad Sci U S A 96:1680-1685.

Naccache L, Dehaene S (2001) The priming method: imaging unconscious repetition priming reveals an abstract representation of number in the parietal lobes. Cereb

Cortex 11:966-974.

Nishitani N, Hari R (2002) Viewing lip forms: cortical dynamics. Neuron 36:1211-1220.

Noesselt T, Hillyard SA, Woldorff MG, Schoenfeld A, Hagner T, Jancke L, Tempelmann C, Hinrichs H, Heinze HJ (2002) Delayed striate cortical activation during spatial attention. Neuron 35:575-587.

Okusa T, Kaneoke Y, Koyama S, Kakigi R (1998) Random dots blinking: a new approach to elucidate the activities of the extrastriate cortex in humans. Neuroreport 9:3961-3965.

Puce A, Allison T, McCarthy G (1999) Electrophysiological studies of human face perception. III: Effects of top-down processing on face-specific potentials. Cereb Cortex 9:445-458.

Raichle ME, Fiez JA, Videen TO, MacLeod AM, Pardo JV, Fox PT, Petersen SE (1994) Practice-related changes in human brain functional anatomy during nonmotor learning. Cereb Cortex 4:8-26.

Ringo JL (1996) Stimulus specific adaptation in inferior temporal and medial temporal

cortex of the monkey. Behav Brain Res 76:191-197.

Rolls ET (2004) Consciousness absent and present: a neurophysiological exploration. Prog Brain Res 144:95-106.

Rolls ET, Tovee MJ, Panzeri S (1999) The neurophysiology of backward visual masking: information analysis. J Cogn Neurosci 11:300-311.

Schacter DL, Buckner RL (1998) Priming and the brain. Neuron 20:185-195.

Schiller PH (1968) Single unit analysis of backward visual masking and metacontrast in the cat lateral geniculate nucleus. Vision Res 8:855-866.

Schoenfeld MA, Woldorff M, Duzel E, Scheich H, Heinze HJ, Mangun GR (2003) Form-from-motion: MEG evidence for time course and processing sequence. J Cogn Neurosci 15:157-172.

Summerfield C, Jack AI, Burgess AP (2002) Induced gamma activity is associated with conscious awareness of pattern masked nouns. Int J Psychophysiol 44:93-100.

Thompson-Schill SL, D'Esposito M, Kan IP (1999) Effects of repetition and competition on activity in left prefrontal cortex during word generation. Neuron 23:513-522.

Turvey MT (1973) On peripheral and central processes in vision: inferences from an information-processing analysis of masking with patterned stimuli. Psychol Rev 80:1-52.

Vanni S, Revonsuo A, Saarinen J, Hari R (1996) Visual awareness of objects correlates with activity of right occipital cortex. Neuroreport 8:183-186.

van Turennout M, Ellmore T, Martin A (2000) Long-lasting cortical plasticity in the object naming system. Nat Neurosci 3:1329-1334.

Wagner AD, Koutstaal W, Maril A, Schacter DL, Buckner RL (2000) Task-specific repetition priming in left inferior prefrontal cortex. Cereb Cortex 10:1176-1184.

Wasaka T, Hoshiyama M, Nakata H, Nishihira Y, Kakigi R (2003) Gating of somatosensory evoked magnetic fields during the preparatory period of self-initiated finger movement. Neuroimage 20:1830-1838.

Wiggs CL, Martin A (1998) Properties and mechanisms of perceptual priming. Curr Opin Neurobiol 8:227-233.

Williams LM, Liddell BJ, Rathjen J, Brown KJ, Gray J, Phillips M, Young A, Gordon E (2004) Mapping the time course of nonconscious and conscious perception of fear:

an integration of central and peripheral measures. Hum Brain Mapp 21:64-74.

Figure 1

Several hypotheses accounting for a BOLD signal decrease in neural adaptation (NA) effect. The neural activity (square function) and predicted BOLD signal (round function, in arbitrary units) in response to a novel (broken line) and repeated (solid line) stimulus are shown in each panel. (A) Activation reduction hypothesis. The decrease in mean firing rate in the repeated condition results in a smaller BOLD amplitude. (B) Shortened duration hypothesis. The stimulus repetition elicits a temporal acceleration of neural processing, which leads to a reduction in the BOLD response. These two models were originally reviewed by Henson and Rugg (Henson and Rugg, 2003), and can be distinguished by a difference in BOLD peak latency, on the assumption that any nonlinear term in the neural-hemodynamic relationship can be excluded. Reprinted from Neurophychologia, vol. 41, Henson and Rugg, 'Neural response suppression, haemodynamic repetition effects, and behavioural priming', pages 263 – 270 and NeuroImage, vol. 15, Henson et al., 'Detecting latency differences in event-related BOLD responses: application to words versus nonwords and initial versus repeated face presentations', pages 83 – 97, Copyright (2002), with permission from Elsevier. (C)

an integration of central and peripheral measures. Hum Brain Mapp 21:64-74.

Figure 1

Several hypotheses accounting for a BOLD signal decrease in neural adaptation (NA) effect. The neural activity (square function) and predicted BOLD signal (round function, in arbitrary units) in response to a novel (broken line) and repeated (solid line) stimulus are shown in each panel. (A) Activation reduction hypothesis. The decrease in mean firing rate in the repeated condition results in a smaller BOLD amplitude. (B) Shortened duration hypothesis. The stimulus repetition elicits a temporal acceleration of neural processing, which leads to a reduction in the BOLD response. These two models were originally reviewed by Henson and Rugg (Henson and Rugg, 2003), and can be distinguished by a difference in BOLD peak latency, on the assumption that any nonlinear term in the neural-hemodynamic relationship can be excluded. Reprinted from Neurophychologia, vol. 41, Henson and Rugg, 'Neural response suppression, haemodynamic repetition effects, and behavioural priming', pages 263 – 270 and NeuroImage, vol. 15, Henson et al., 'Detecting latency differences in event-related BOLD responses: application to words versus nonwords and initial versus repeated face presentations', pages 83 – 97, Copyright (2002), with permission from Elsevier. (C)

Integrative model of the response attenuation and temporal acceleration proposed in the present study. The repetition of the same stimulus produces a more rapid and smaller neural response in this model. The temporal duration is, however, not affected by the stimulus repetition. The reference function of hemodynamics was adopted from Friston et al. (Friston et al., 1998).

Figure 2

Schematic illustration of the stimulus presentation paradigm used in experiment 1. (A) The random-dot blinking (RDB) method for the presentation of letter stimuli. Capital letters were presented through a 60 x 60 random dot field in the central visual field, although the number of dots is reduced in this figure. While each dot in the field is vibrating at 60 Hz in the resting period (left panel), the dynamic-static segregation of dots elicits a perception of visual letters in the character presentation period (middle panel). The contour of 'A' depicted by the thick line is shown only for this illustration. The actual density of the dot is shown in the right panel. In this figure, stimulus images of four consecutive frames during the presentation are overlaid to illustrate the dynamic and static texture. The dots in the static texture stay at the same place, thus their overlaid image appears solid. On the other hand, the overlaid dynamic dots show

various appearances due to the dot motion. (B) The event charts in the SINGLE and three ISI conditions. While only S1 (300 ms) was presented in the SINGLE condition, S1 (300 ms) and S2 (500 ms) were sequentially presented in the ISI 150, 250, and 350 conditions. In all conditions, the averaging epoch of MEG signal was from –100 ms to 1200 ms relative to the S1 onset.

Figure 3

MEG signals of a representative subject. (A) VEF waveforms over 204 planar coils in the SINGLE condition. (B) The superimposed waveform of 33 SOIs in the same subject. (C) MEG waveforms in two SOIs encompassed in panel A. In addition to the MEG signals in the SINGLE condition (black line), waveforms in the other six conditions are also shown in this panel. The blue, green, and red lines correspond to VEFs in the ISI 150, 250, and 350 conditions, respectively. For each ISI condition, the data in the 'SAME' (solid line) and 'DIFF' (broken line) trials were plotted. All data in A-C were digitally filtered (0.1-30 Hz bandpass) for display purposes.

Figure 4

Anatomical location of the signal source in the SINGLE condition. (A) The ECD

location estimated at the peak of the large component shown in Figure 3B. The mean dipole coordinates (5 and 7 dipoles in the left and right hemisphere, respectively) across subjects were plotted on the MR image of a representative subject. (B) The distribution of SOIs across 10 subjects. The number of SOIs in each sensor position was summed across subjects and color-coded on a contour map depicted over the topographical layout of 102 sensor positions. (C) MEG signal strength at 300 ms of the SINGLE waveform. Same as B, but the mean deflection across ten subjects were represented in this map. The data in two planar sensors (latitudinal and longitudinal) were averaged for each position. Note that both topographical maps (B and C) show the distinct neural responses in bilateral occipito-temporal regions.

Figure 5

Across-SOI waveforms of seven conditions. The data for one representative subject (A), grand mean waveforms of 10 subjects (B), and normalized grand mean timecourses (C) are shown. In C, the peak amplitude of S2 response in each paired-stimulus condition was represented as 1. As Figure 3C, the blue, green, and red lines represent ISI 150, 250, and 350 conditions (solid: SAME, broken: DIFF). The event charts for the three ISI conditions are also displayed below each timeseries.

Figure 6

Statistic comparisons of brain responses between the SAME and DIFF trials. For both S1 (A, C, E) and S2 (B, D, F) responses, three parameters were calculated from across-SOI waveform of each subject: peak amplitude (A, B), peak latency (C, D), and FWHM (E, F). The blank and filled bars indicate the data in the SAME and DIFF trials, respectively. Error bars denote the SE across 10 subjects. Note that peak latency to S2 (panel D) was measured from the S2 onset in each ISI condition.

Figure 7

The repetition effects measured by three indices. The differences between DIFF-SAME were shown for each parameter; peak amplitude (A), peak latency (B) and FWHM (C). Error bars denote the SE across 10 subjects. * $P < 0.05$, ** $P < 0.01$, one group t-test.

Figure 8

The relationship between behavioral data and MEG waveforms. (A) The RT data in the vowel/consonant judgment task measured from the S2 onset. As in Figure 6, the

blank and filled bars indicate the data in the SAME and DIFF trials and error bars denote the SE across 10 subjects. *** $P < 0.0001$, paired t-test. (B) Correlation analyses of the RT data with two temporal parameters of MEG response: S2 peak latency (Fig. 6D**)** and FWHM (Fig. 6F**)**. The data for six conditions in ten subjects (60 points) were plotted for each parameter. A significantly high correlation was observed between RT and peak latency (represented as ●, $r = 0.48$, $P < 0.0001$, significance test for correlation coefficients), but not between RT and FWHM of the S2 response (○, r = 0.09, $P > 0.05$). (C) Same as B, but the difference of SAME and DIFF (DIFF – SAME) in each ISI of each subjects were compared between RT and peak latency or FWHM (thus, 30 points were plotted for each parameter).

Figure 9

Random-dot blinking (RDB) method and event charts in experiment 2. (A) The RDB method for the presentation of visual stimuli. Visual patterns were depicted in a 60 x 60 random dot field at the central visual field, although the number of dots is reduced in this figure. While all dots in the field are vibrating at 60 Hz in the resting period (left panel), the dynamic-static segregation of dots elicits a perception of visual patterns in the stimulus presentation period (right panel). The contour of ‘m’ depicted by the

thick line is shown only for this illustration. (B) The target (left and middle panel) and mask (right panel) patterns used in the present study. In the experiment, all patterns were depicted by the RDB method shown in panel A. (C) The event charts of the five conditions. While the target and mask were sequentially presented in three ISI conditions (ISI 0, ISI 150, and ISI 300), only either the target or the mask was shown in two control conditions (TGT and MSK). In all conditions, the averaging epoch of MEG signal was from –200 ms to 1300 ms relative to the target onset.

Figure 10

Task performance in paired-stimuli conditions. Error bars denote the standard error (SE) across subjects. Taking into account the inter-subject variability, the behavioral data in the three ISI conditions were normalized to the accuracy in the TGT condition of each subject. The actual values (%) were given in the text (see Results) * $P < 0.05$, post-hoc test with Bonferroni correction.

Figure 11

Neuromagnetic responses and their source locations. (A) MEG signals of a representative subject. The VEF waveforms over 204 planar coils in the MSK

condition were plotted except for one sensor that showed a low signal-to-noise ratio on that day. (B) The superimposed waveform of 29 sensors selected in the same subject as A. All data in A and B were digitally filtered (0.1-30 Hz bandpass) for display purposes only.

Figure 12

Anatomical location of the neuromagnetic signal. (A) The equivalent current dipole (ECD) location estimated at the peak of the large component in Figure 11B. The mean coordinates across 6 subjects were plotted on the MR image of a representative subject. (B) The distribution of SOIs across 11 subjects. The number of selected sensors in each measurement position was summed across subjects and color-coded on a contour map depicted over the topographical layout of 102 sensor positions.

Figure 13

Time series in occipito-temporal activities. Across-sensor waveforms in two representative subjects and grand average of 11 subjects. The waveforms in two single-stimulus conditions (TGT: thin, MSK: thick) and three paired-stimuli conditions (ISI 0: blue, ISI 150: green, ISI 300: red) are presented in the upper and lower panels,

respectively. The event chart for each condition is also displayed below each time series. The duration of the target was 100 ms for Subject 1 and 150 ms for Subject 2. The neural responses to the mask (indicated by arrows in lower panels) shift rightward along with the increase in ISI.

Figure 14

Isolated neural responses to the target stimuli. (A) The neuromagnetic waveforms (N = 11) in the three ISI and TGT conditions. The waveform in the MSK condition was subtracted from that for each of the three ISI conditions with the difference in presentation timing of the mask corrected. The right panel shows averaged (N = 11) time courses aligned to the peaks of ISI 0 – MSK waveforms in each subject. The zero in the abscissa of this panel indicates the peak latency of the ISI 0 – MSK condition. (B) Bar graphs of peak amplitude (left) and latency (right) of the target responses. Error bars denote the SE across 11 subjects.

Figure 15

Correlation analyses of the task accuracy with two indices of MEG: the peak amplitude (left) and peak latency (right). The data of four conditions (TGT, ISI 0, 150, and 300)

in 10 subjects whose behavior data were successfully recorded were plotted for each parameter. *** $P < 0.001$, significance test for correlation coefficients.

Figure 16

Comparison of correct and incorrect trials. (A) Time series of neural waveforms in correct (thick line) and incorrect (thin line) trials in ISI 0 condition. (B) Bar plots of mean (± SE across subjects) peak amplitude and latency. Correct trials (filled bars) showed significantly larger peak amplitude than incorrect trials (blank bar), while no significant difference was observed in peak latency. * $P < 0.05$, paired t-test.

Figure 17

Neuromagnetic responses in occipito-temporal (left column) and anterior temporal (right column) regions. (A) Distribution of selected sensors in each region. (B) Subtracted time series in four conditions. (C) Peak amplitude. (D) Peak latency. In all of four panels in (C) and (D), one-way ANOVA indicated a significant main effect of conditions (occipito-temporal region, peak amplitude: $F = 15.26$, $P < 0.001$, peak latency: $F = 12.44$, $P < 0.001$, anterior temporal region, peak amplitude: $F = 31.99$, $P < 0.001$, peak latency: $F = 8.15$, $P < 0.05$).

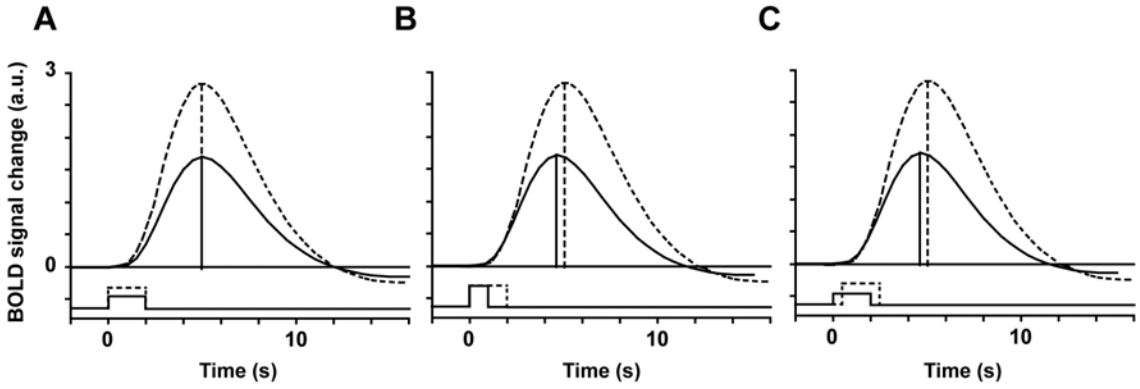

Figure 1

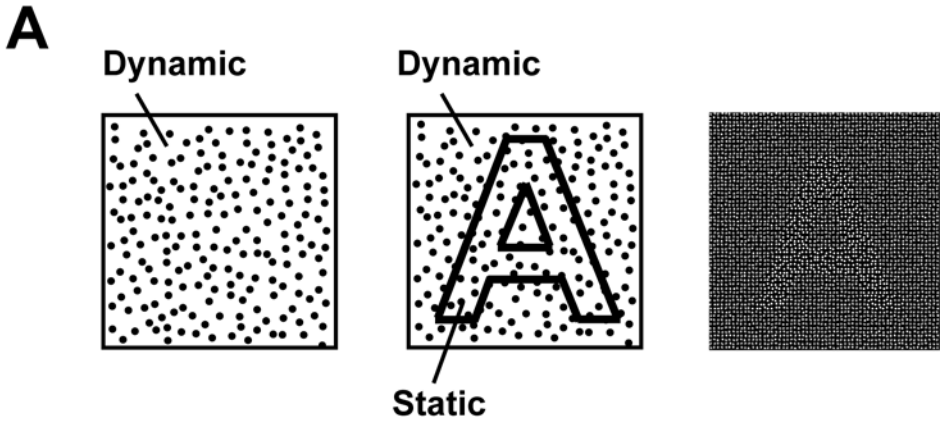
A
Dynamic
Dynamic
Static

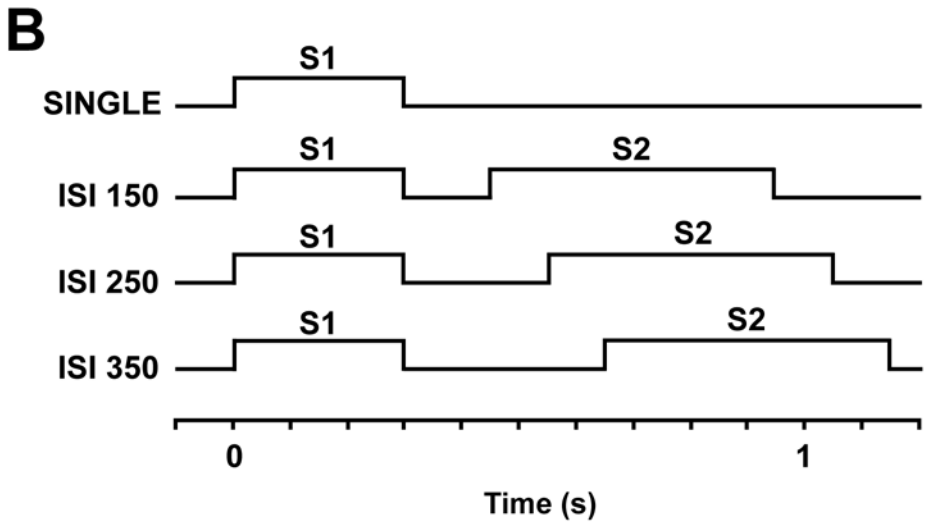
B
S1
SINGLE
S1
S2
ISI 150
S1
S2
ISI 250
S1
S2
ISI 350
0
1
Time (s)

Figure 2

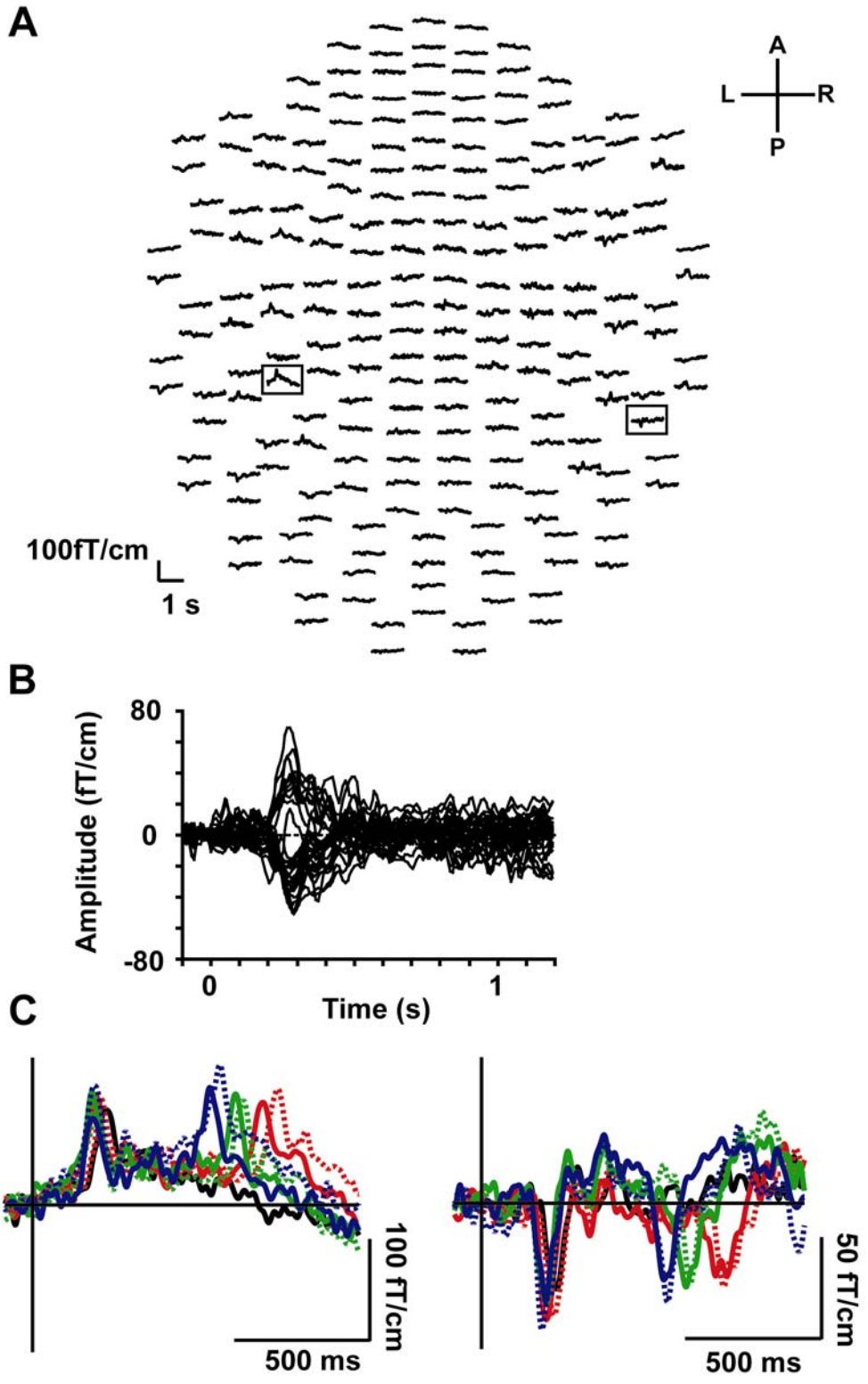
A
A
L
R
P
100fT/cm
1 s
B
80
0
-80
Amplitude (fT/cm)
0
1
Time (s)
C
100 fT/cm
500 ms
50 fT/cm
500 ms

Figure 3

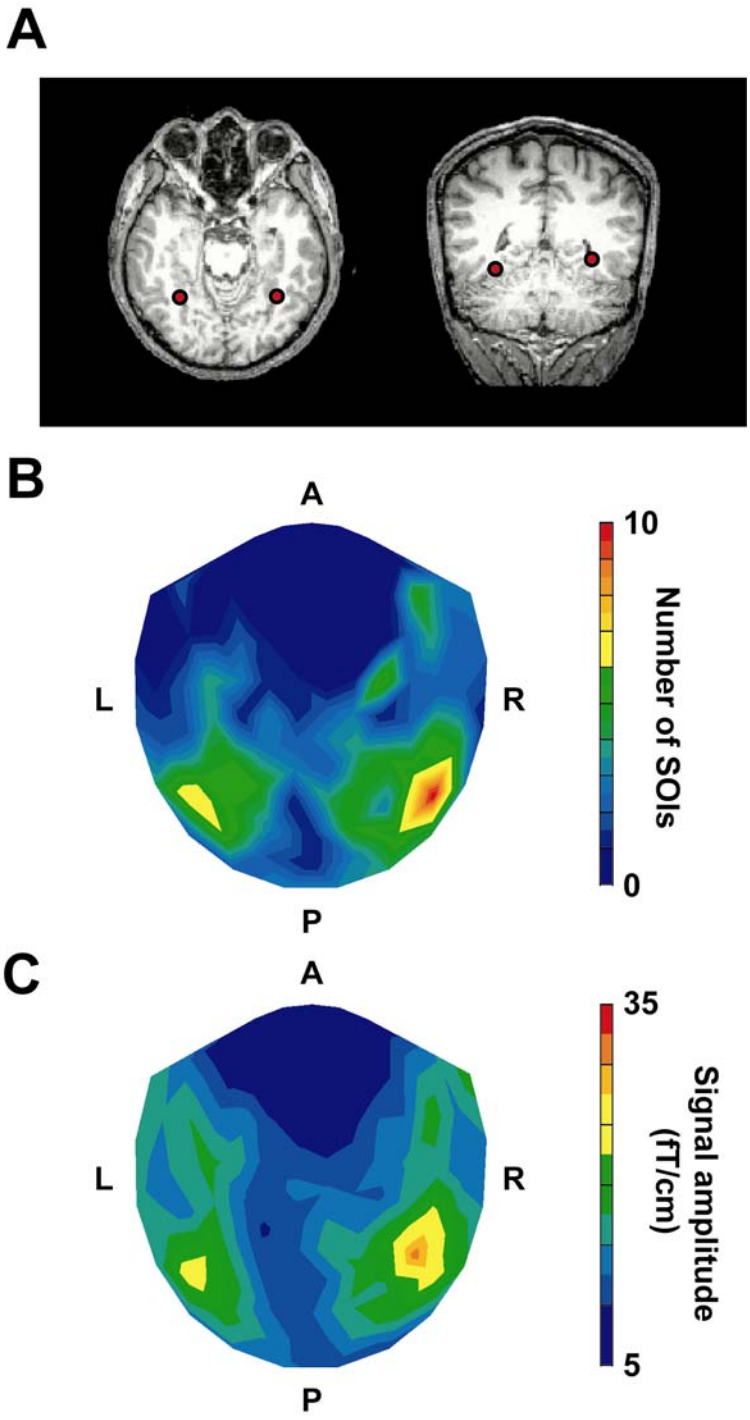

Figure 4

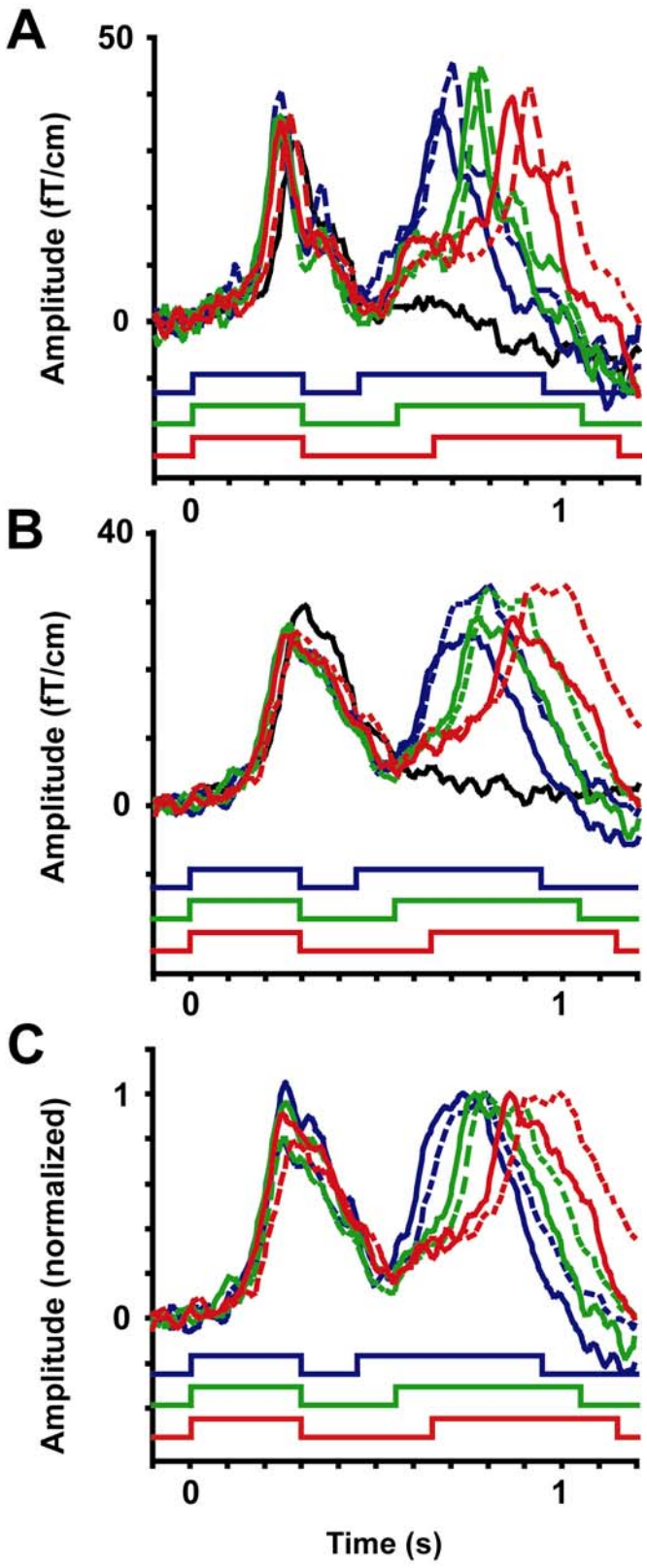
A
50
0
Amplitude (fT/cm)
0
1
B
40
0
Amplitude (fT/cm)
0
1
C
1
0
Amplitude (normalized)
0
1
Time (s)

Figure 5

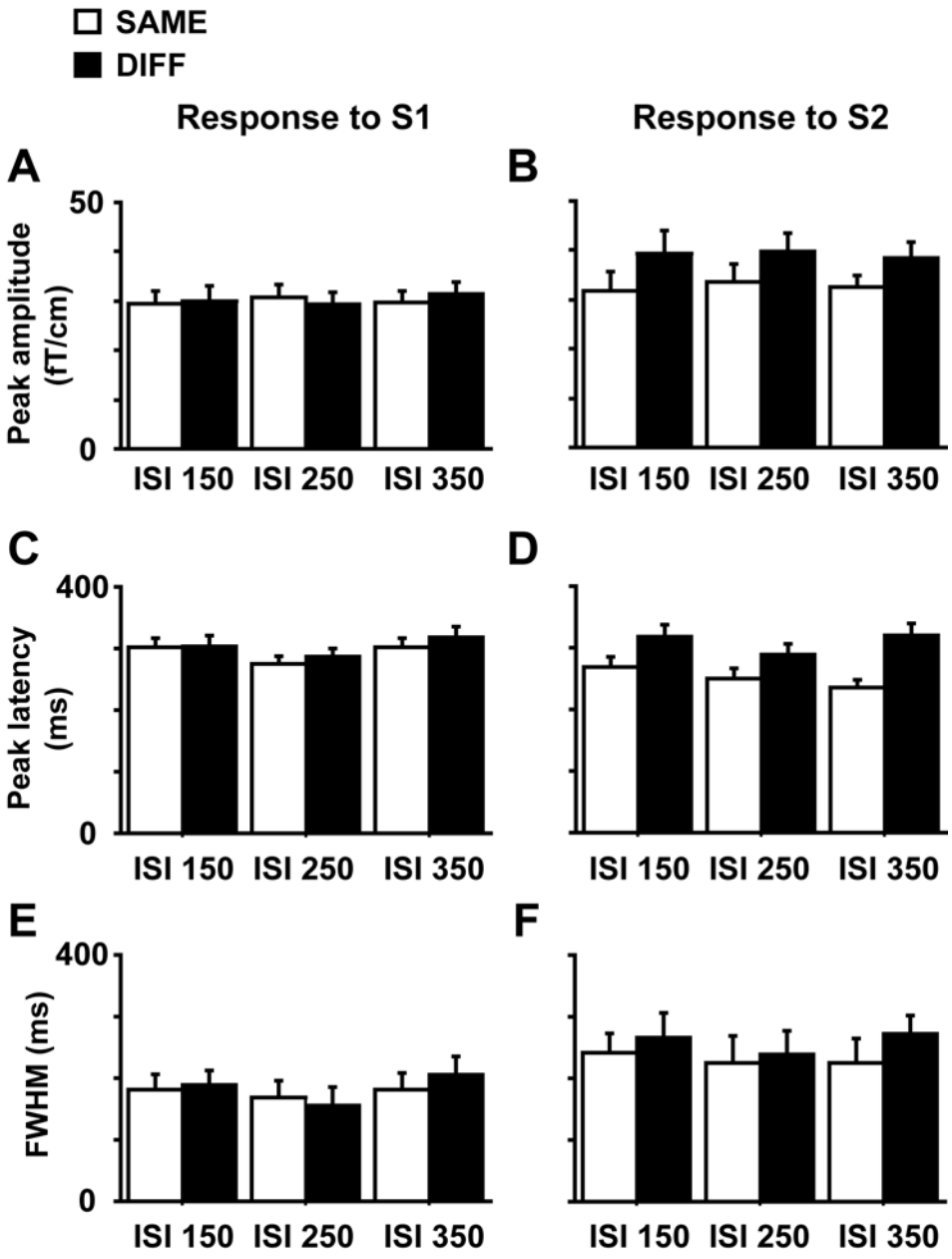
SAME
DIFF
Response to S1
Response to S2
A
B
C
D
E
F
Peak amplitude (fT/cm)
Peak latency (ms)
FWHM (ms)
50
400
0
ISI 150
ISI 250
ISI 350

Figure 6

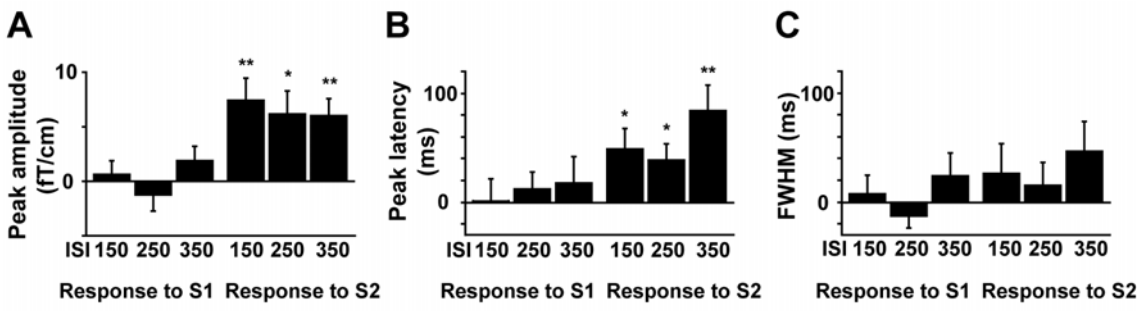
A
Peak amplitude (fT/cm)
10
0
**
*
**
ISI 150 250 350 150 250 350
Response to S1 Response to S2
B
Peak latency (ms)
100
0
*
*
**
ISI 150 250 350 150 250 350
Response to S1 Response to S2
C
FWHM (ms)
100
0
ISI 150 250 350 150 250 350
Response to S1 Response to S2

Figure 7

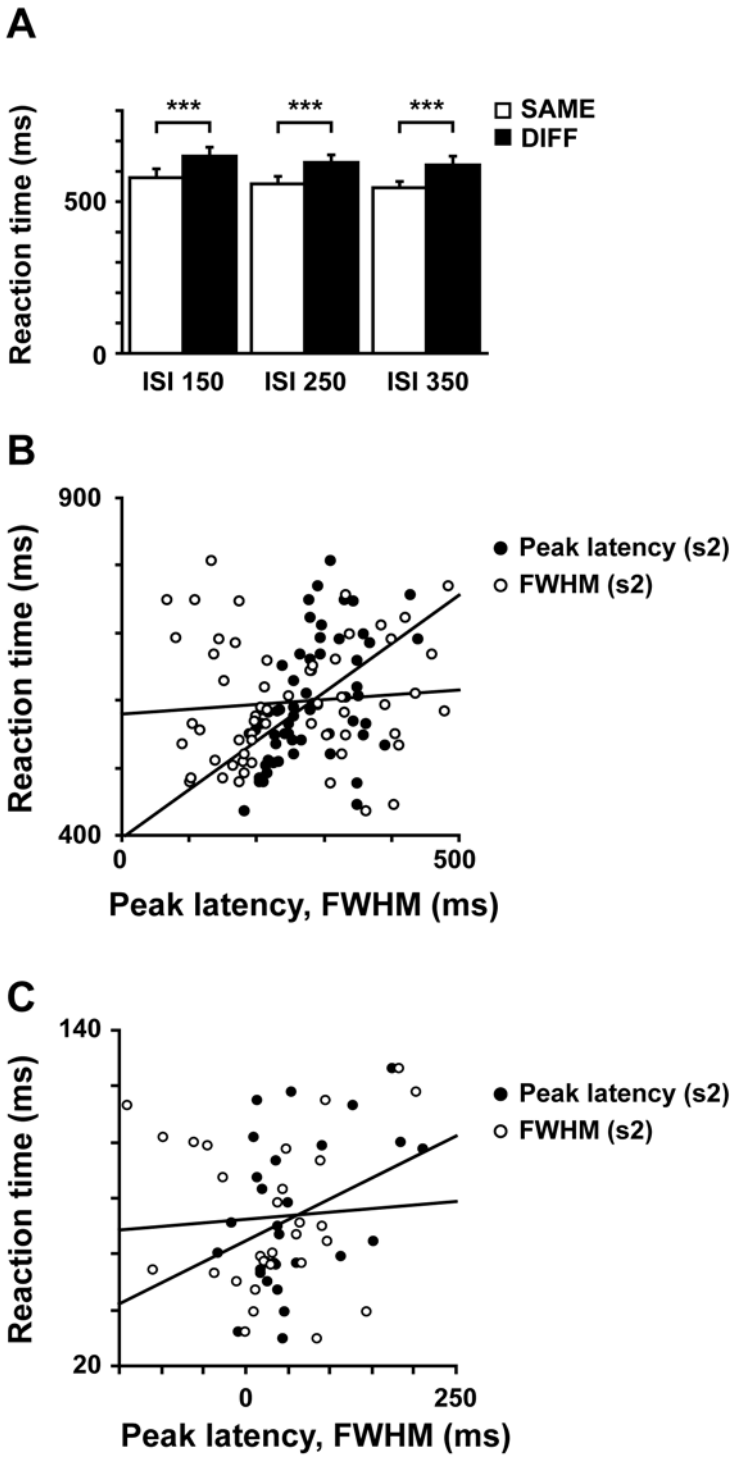
A
***
***
***
SAME
DIFF
Reaction time (ms)
500
0
ISI 150
ISI 250
ISI 350
B
900
400
Reaction time (ms)
Peak latency (s2)
FWHM (s2)
0
500
Peak latency, FWHM (ms)
C
140
20
Reaction time (ms)
Peak latency (s2)
FWHM (s2)
0
250
Peak latency, FWHM (ms)

Figure 8

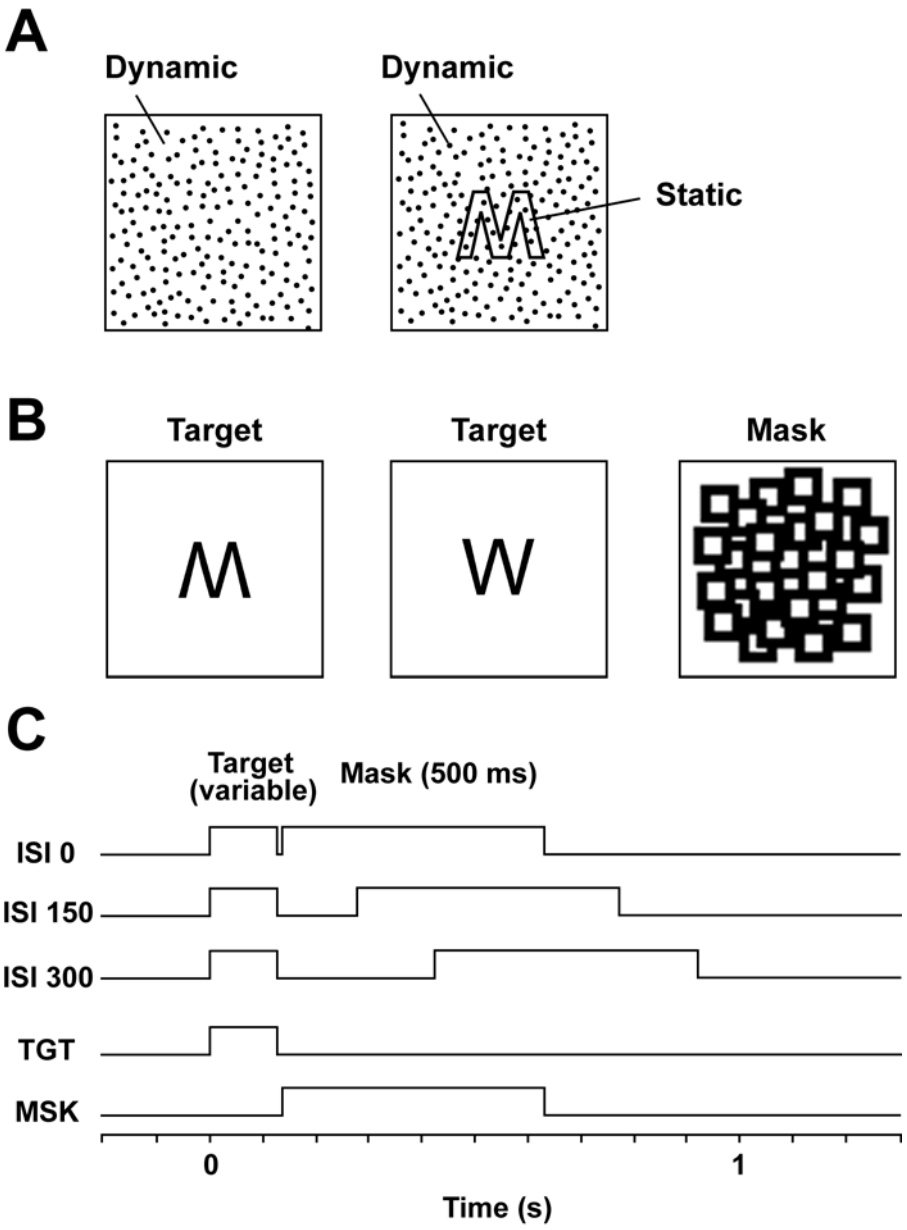
A
Dynamic
Dynamic
Static
B
Target
Target
Mask
M
W
C
Target
(variable)
Mask (500 ms)
ISI 0
ISI 150
ISI 300
TGT
MSK
0
1
Time (s)

Figure 9

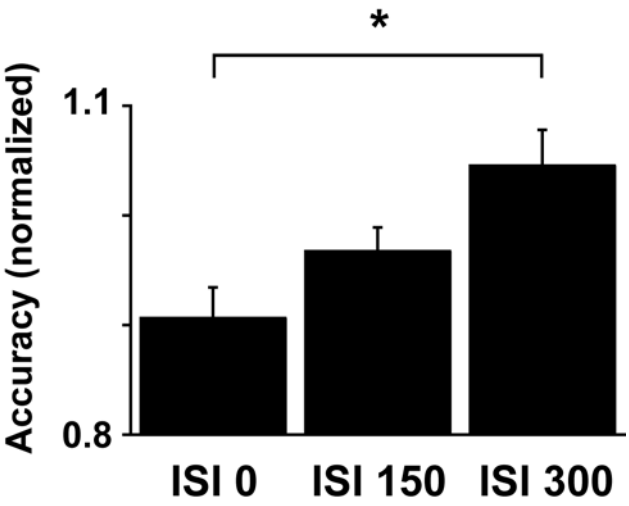

Figure 10

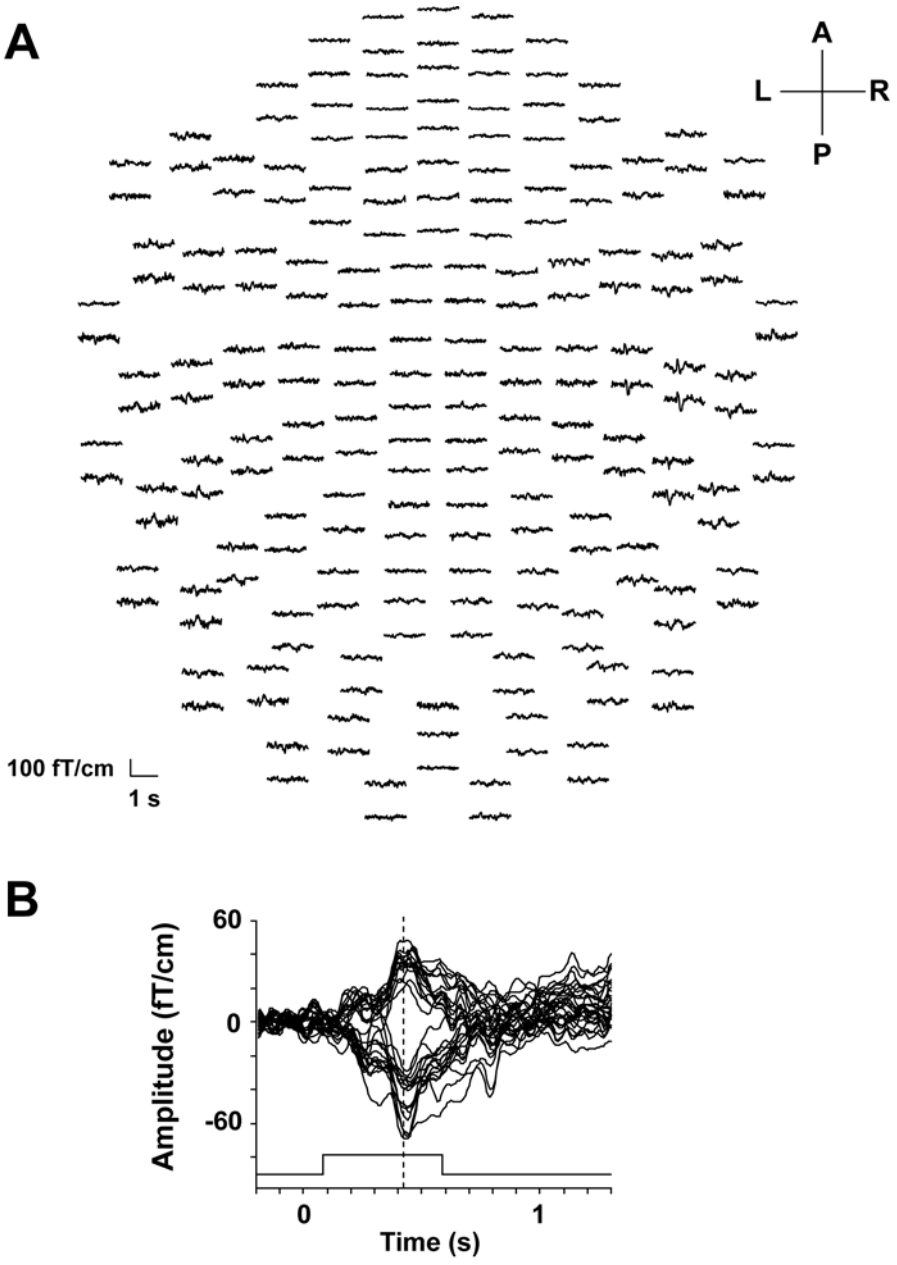

Figure 11

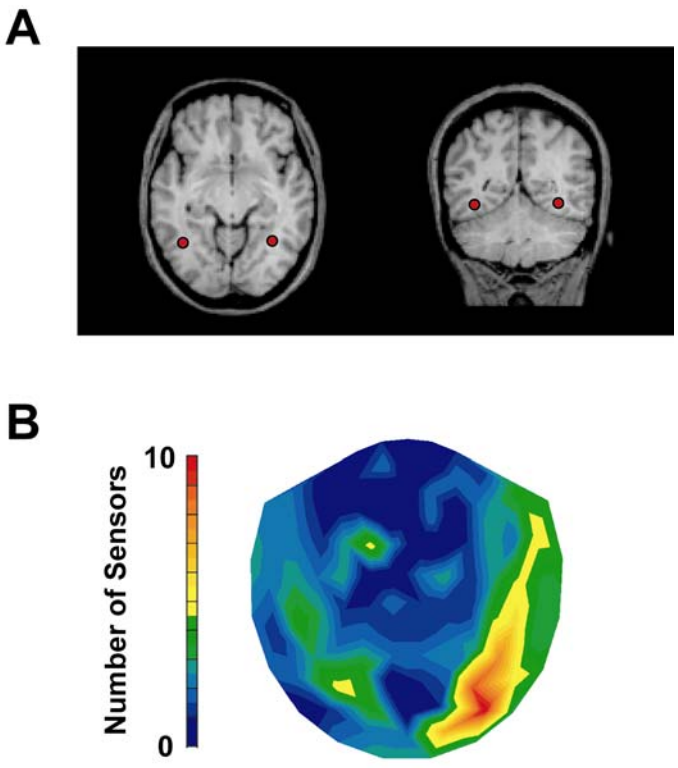

Figure 12

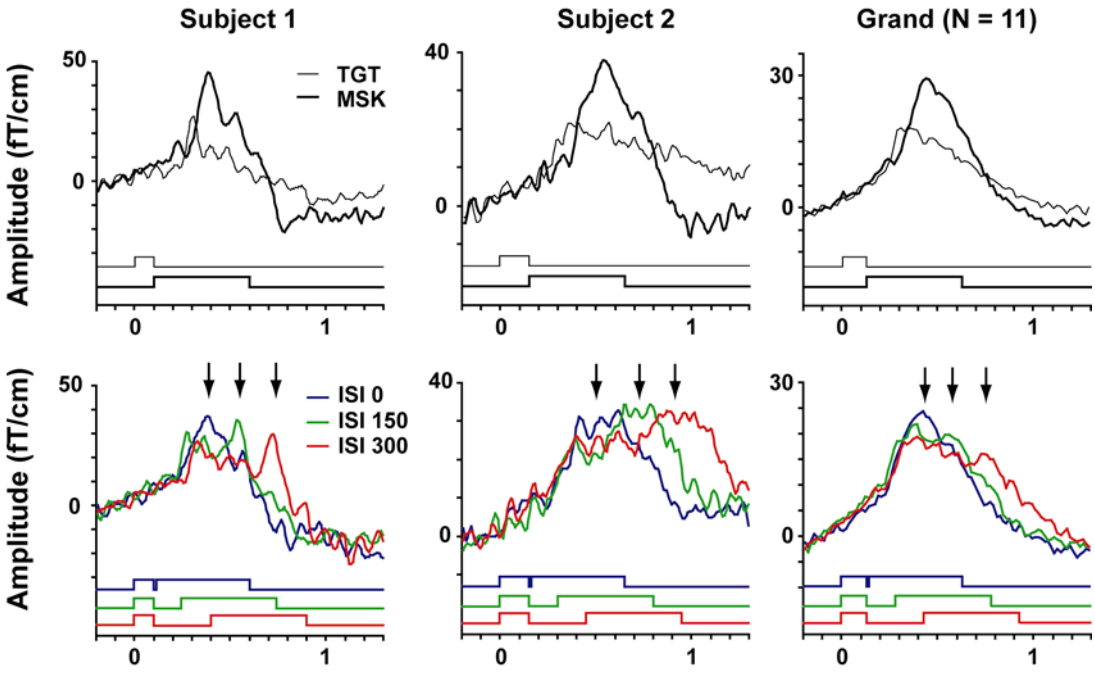
Subject 1
Subject 2
Grand (N = 11)
Amplitude (fT/cm)
TGT
MSK
ISI 0
ISI 150
ISI 300
50
40
30
0
1

Figure 13

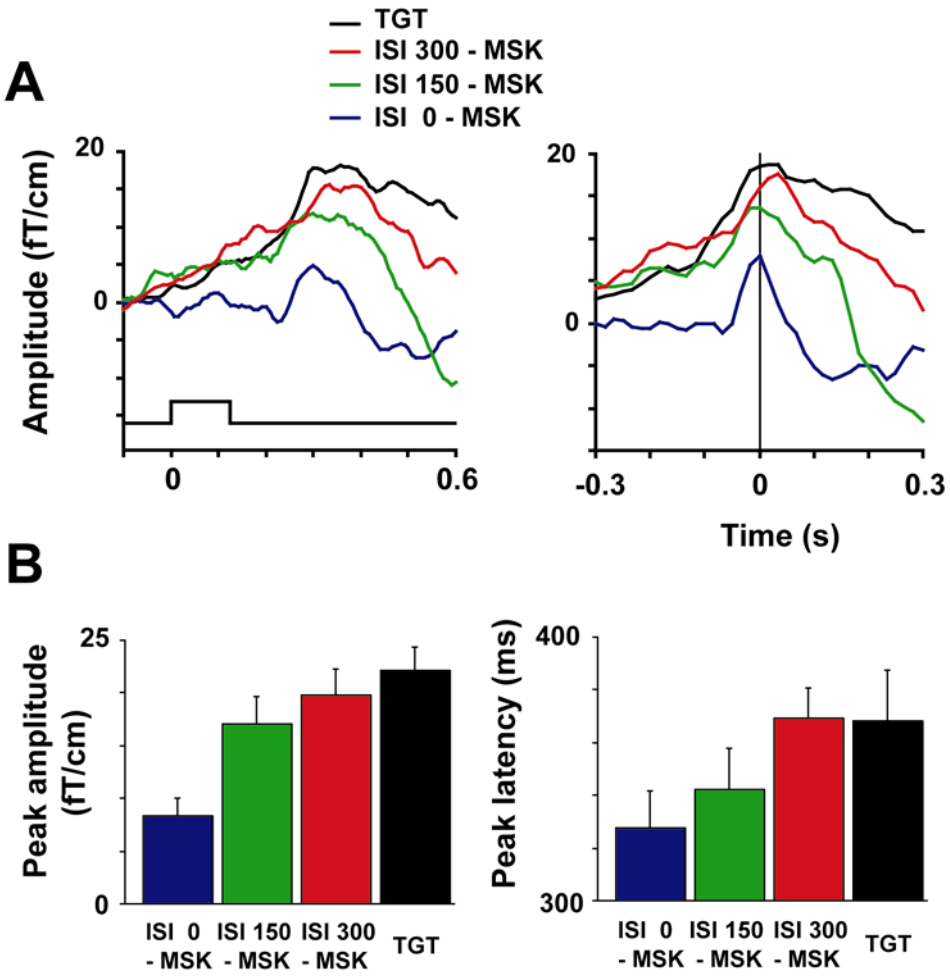
A
TGT
ISI 300 - MSK
ISI 150 - MSK
ISI 0 - MSK
Amplitude (fT/cm)
20
0
0
0.6
20
0
-0.3
0
0.3
Time (s)
B
Peak amplitude (fT/cm)
25
0
ISI 0 - MSK
ISI 150 - MSK
ISI 300 - MSK
TGT
Peak latency (ms)
400
300
ISI 0 - MSK
ISI 150 - MSK
ISI 300 - MSK
TGT

Figure 14

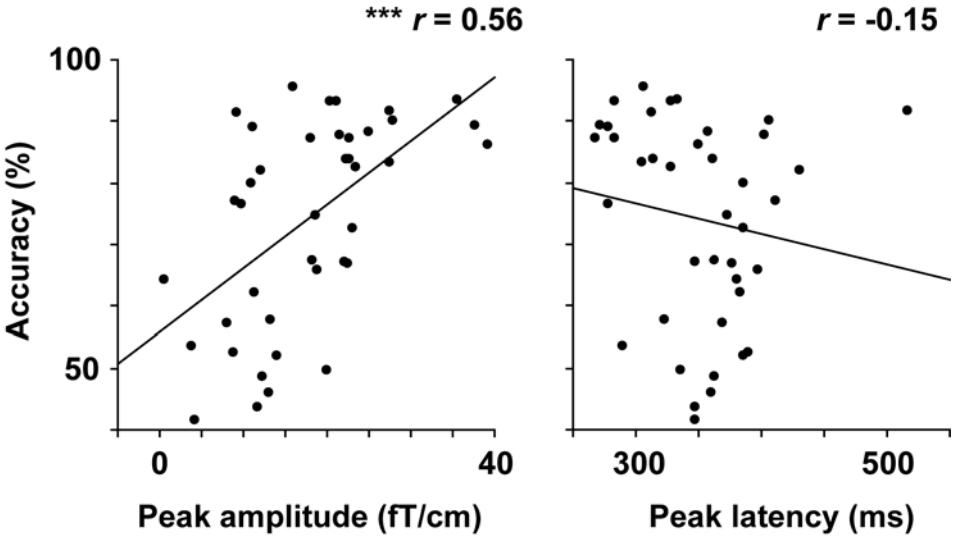
*** r = 0.56
r = -0.15
100
50
Accuracy (%)
0
40
300
500
Peak amplitude (fT/cm)
Peak latency (ms)

Figure 15

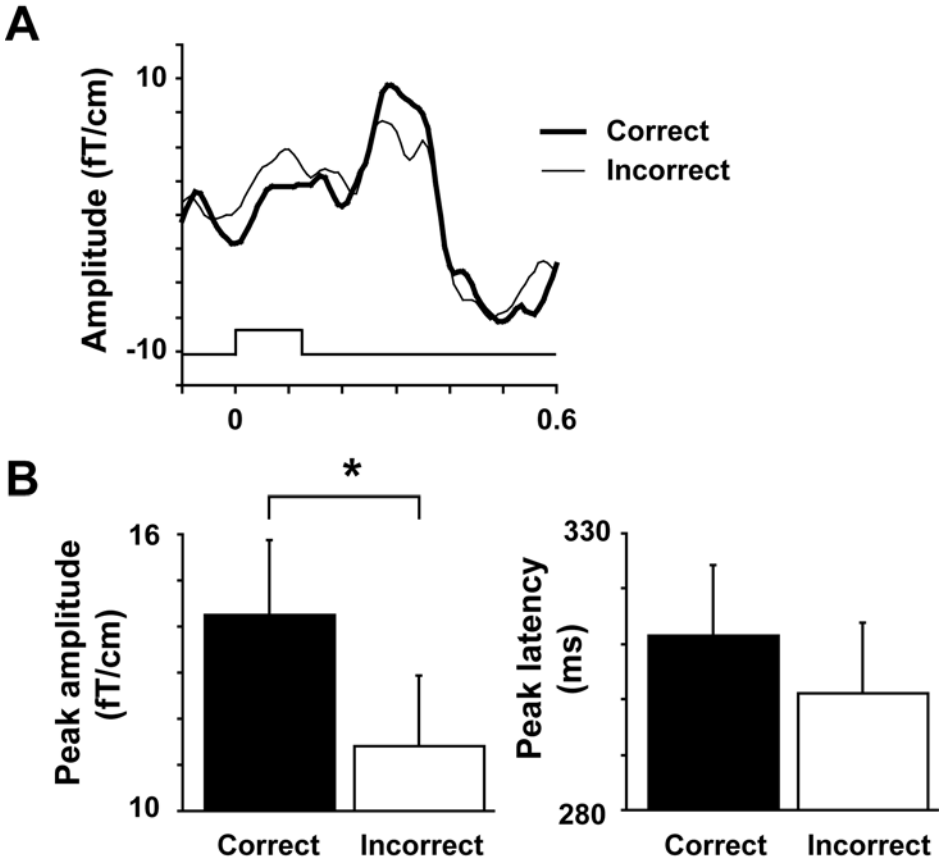
A
10
-10
Amplitude (fT/cm)
0
0.6
Correct
Incorrect
B
*
16
10
Peak amplitude (fT/cm)
Correct
Incorrect
330
280
Peak latency (ms)
Correct
Incorrect

Figure 16

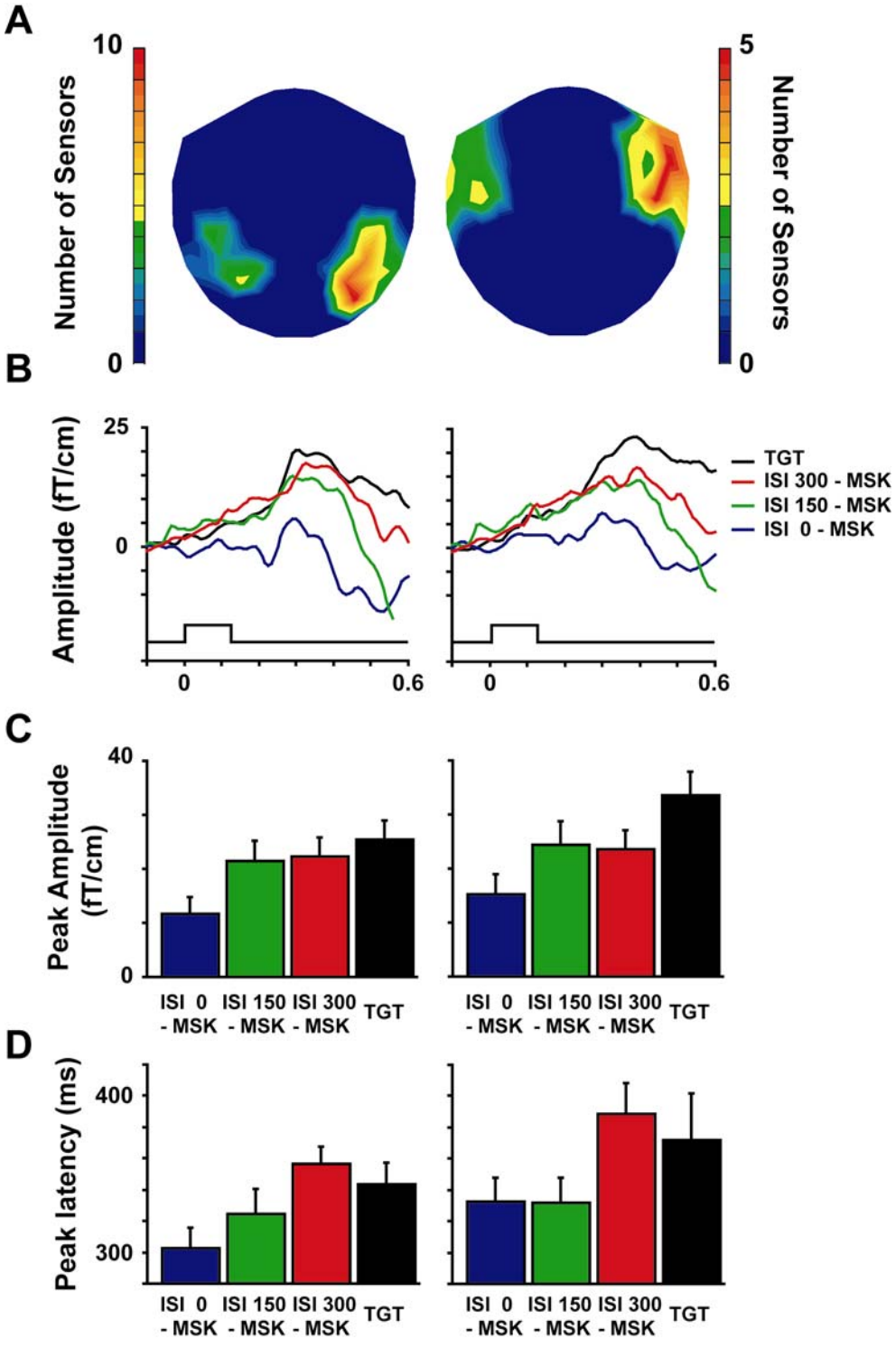
A
10
0
Number of Sensors
5
0
Number of Sensors
B
25
0
Amplitude (fT/cm)
0
0.6
0
0.6
TGT
ISI 300 - MSK
ISI 150 - MSK
ISI 0 - MSK
C
40
0
Peak Amplitude (fT/cm)
ISI 0 - MSK
ISI 150 - MSK
ISI 300 - MSK
TGT
ISI 0 - MSK
ISI 150 - MSK
ISI 300 - MSK
TGT
D
400
300
Peak latency (ms)
ISI 0 - MSK
ISI 150 - MSK
ISI 300 - MSK
TGT
ISI 0 - MSK
ISI 150 - MSK
ISI 300 - MSK
TGT

Figure 17